



Faculty of Science and Technology

MASTER'S THESIS

Study program/ Specialization: Petroleum technology	Spring semester, 2013 Restricted access
Writer: Lars Uglebakken (Writer's signature)
Faculty supervisor: Mesfin Belayneh - UiS External supervisor: Ola M. Vestavik - Reelwell	
Titel of thesis: Reelwell Drilling Method - Installation and cementation of 10 ¾" casing and 7" liner - method and case example.	
Credits (ECTS): 30	
Key words: Casing, Liner, installation, cementing, Reelwell Drilling Method, simulation	Pages: 55 + enclosure:17 Stavanger, 14.06.2013

ABSTRACT

Current technology gives an opportunity to drill Extended Reach Drilling (ERD) wells with a tremendous length of horizontal departure. The Reelwell Drilling Method (RDM) is a drilling technology particularly suited for such long reach wells. This technology gives an opportunity to limit the impact on the environment and reduce the costs. However, to drill ERD wells effectively requires significant improvements in drilling fluids, pressure management, cuttings transport, and mechanical performance of the drillstring.

This thesis presents a simulation study the challenges regarding mechanical loads and pressure management for installation and cementation of 10 ³/₄ casing 7". For the study, a 15,800 m Measured Depth (MD) ERD well which is planned to be drilled by the RDM was considered.

The main objective of the study is to provide an advice for the feasibility of the RDM technology, which is under research and development phase. The study was performed with Landmark WELLPLANTM commercial simulator and literature based theory implemented in MATLAB.

The results of the study summarize as follows:

- For installation:
 - The simulation result shows that the drag forces under tripping in or tripping out can be kept within the buckling and tensile limit. This is done by controlling friction coefficient and the operation parameters such as RPM and running speed.
- For cementing:
 - By the use of standard cementing fluids (cement slurry, spacer, and mud), the simulation results show well integrity problems. Even at very low rates the formation will fracture.
 - The cementing operation can safely be done by controlling the Equivalent Circulating Density (ECD). This can be controlled by reducing the fluid flow rate, reduce the length of the cemented section, and by the use of low density and/or low viscosity cementing fluids. The lower density and viscosity cementing fluids can even be circulated at very high flow rates without well integrity problem.

ACKNOWLEDGEMENTS

This thesis is the concluding part of my master degree in Petroleum Engineering at the Faculty of Science and Technology at the University of Stavanger. It is carried out in cooperation with Reelwell. The work has been limited to the period between January - June 2013.

Working with this thesis has been very interesting, challenging and it has given me a great learning experience.

I would like to thank my faculty supervisor Mesfin Belayneh for great amount of help with the thesis and for all the good feedback. I would also thank my external supervisor Ola M. Vestavik and his colleagues at Reelwell for all the good advice and guidance during the spring. A special thanks to Lars Alfors at Halliburton for his help regarding the simulation software and fluid data.

Lastly, I would like to thank my friends and family for all their support throughout the five years of studies at the University of Stavanger.

TABLE OF Content

ABSTRACT	ii
ACKNOWLEDGEMENTS.....	iii
ABBREVIATIONS	vi
LIST OF FIGURES	vii
1 INTRODUCTION.....	1
1.1 Background.....	1
1.2 Objective	2
2 REELWELL Technology	3
2.1 Reelwell Drilling Method (RDM) vs. Conventional systems	3
2.2 Components of the RDM system	3
3 Literature study for simulation and installation procedure.....	6
3.1 Fluid rheology models	6
3.1.1 Bingham Plastic Model	6
3.1.2 Power Law Model.....	7
3.1.3 Herschel-Bulkley	7
3.2 Pressure losses	8
3.2 Equivalent circulating density	9
3.3 Frictional pressure loss.....	9
3.3 Torque and drag	10
3.3.1 Drag	10
3.3.2 Torque model	11
3.4 Running and cementing of liner	11
3.4.1 Conventional running and cementing of liner.....	11
3.4.2 Field Case study – Visund Field in the North Sea	13
4 Simulation study using Landmark WELLPLAN	15
4.1 Simulation study installation and cementation of 10 ¾” casing.....	15
4.1.1 Simulation of 10 ¾” casing installation	15
4.1.1.1 Simulation arrangement.....	15
4.1.1.2 Simulation result	17
4.1.2 Simulation of cementation 10 ¾” casing	21
4.1.2.1 Simulation arrangement.....	21
4.1.2.2 Simulation result	23

4.2 Simulation study installation and cementation of 7" casing	28
4.2.1 Simulation of installation 7" casing.....	29
4.2.1.1 Simulation arrangement.....	29
4.2.1.2 Simulation result	30
4.2.2 Simulation of cementation 7" casing	34
4.2.2.1 Simulation arrangement.....	34
4.2.2.2 Simulation result	35
5 Simulation study of cementation of 10 3/4" casing using MATLAB	38
5.1 Simulation arrangement.....	38
5.2 Simulation results	38
6 Summary and discussion	45
7 Further work	46
References	47
Appendix A: Hydraulics models	49
A.2 Bingham Plastic fluid	49
A.3 Power law fluid.....	49
A.4 Herschel-Bulkley fluid	50
A.4 Newtonian fluid.....	51
Appendix B: Simulated well geometry and survey	53
B1: Survey	53
B2: Vertical well section	53
B3: Horizontal well section.....	54
B4: Dogleg Severity.....	54
Appendix C MATLAB code	55
Appendix D Review of cementing	62

ABBREVIATIONS

The following abbreviations are used in this thesis:

Abbreviation	Definition
ECD	Equivalent Circulating Density
ERD	Extended Reach Drilling
ID	Inner Diameter
MD	Measured Depth
OD	Outer Diameter
PPF	Pound per Feet
RDM	Reelwell Drilling Mehtod
RPM	Revolutions per Minute
s.g.	specific gravity
TVD	True Vertical Depth

LIST OF FIGURES

Fig 1.1 The RDM makes it possible to extend the horizontal reach. (Reelwell).....	2
Fig 2.1 Comparisons of conventional drilling and Reelwell technology (Reelwell).....	3
Fig 2.2 components of the RDM system.....	4
Fig 2.3 schematic of the equipment arrangement for the RDM (Belarde & Vestavik, 2011)...	5
Fig 3.1 Illustration of rheology behavior (Pacific Northwest National Laboratory).....	6
Fig 3.2 schematic of the pressure losses during circulation (H. Rabia, 1985).....	8
Fig 3.3 schematic of a segmented drill string.....	10
Fig 3.4 schematic of liner setting tool and hanger assembly(Nelson & Guillot, 2006).....	13
Fig 4.1 Schematic of hole section and drill string arrangement.....	16
Fig 4.2 Vertical section of the well.....	17
Fig 4.3 Effective tension by tripping in/out for various RPM.....	18
Fig 4.4 Effective tension by tripping in/out for various RPM.....	19
Fig 4.5 Effective tension for 20 RPM and 40 RPM.....	19
Fig.4.6 Effective tension for various friction factors.....	21
Fig.4.7 Pore and Fracture pressure.....	22
Fig 4.8 Schematic figure of the cementing job.....	23
Fig 4.9 Maximum downhole pressure profile for the cement job for displacement at 1,000 l/min.....	24
Fig 4. 10 Maximum ECD for various flow rates.....	25
Fig 4.11 Maximum downhole pressure profile for the cement job for displacement at 1,000 l/min.....	26
Fig 4.12 Maximum ECD for various flow rates.....	27
Fig 4.13 Maximum cemented section for different flow rates.....	28
Fig 4.14 Maximum cemented length for different flow rates.....	28
Fig 4.15 Schematic of hole section and drill string arrangement.....	29
Fig 4.16 Vertical section of the well.....	30
Fig 4.17 Effective tension by tripping in/out for various RPM.....	31
Fig 4.18 Effective tension for various RPM.....	32
Fig 4.19 Effective tension by tripping in/out for various friction coefficients.....	33
Fig 4.20 Pore and Fracture pressure.....	34
Fig 4.21 Schematic figure of the cementing job.....	35
Fig 4.22 Maximum ECD for different flow rates.....	36
Fig 4.23 Maximum ECD for different flow rates.....	37
Fig 4.24 ECD for three different rheology models.....	40
Fig 4.25 ECD for three different rheology models.....	42
Fig 4.26 ECD for three different rheology models.....	44

1 INTRODUCTION

The first commercial directional drilling technology was developed in 1929, to drill wells from an onshore rig to exploit oil reserves beneath the ocean. The technology has developed through the years and greatly increased the horizontal departure of the wells. (Mitchell & Miska, 2011). A well that have an along-hole departure of more than twice the True Vertical Depth (TVD) is often defined as an Extended Reach Drilling (ERD) well (Agbaji, 2010).

ERD wells gives an opportunity to reduce the number of drilling locations, reach inaccessible target areas, access offshore reservoir from onshore rigs, and limit the impact on the environment (Devereux, 2012) (Mason & Judzis, 1998).

However, as horizontal departure is increased as a result of improved technology, the challenges are getting tougher. To drill ERD wells effectively requires significant improvements in drilling fluids, pressure management, cuttings transport, and mechanical performance of the drillstring (Mitchell & Miska, 2011).

This thesis will study the challenges regarding mechanical loads and pressure management for installation and cementation of casing and liner for an ERD well, drilled by the Reelwell Drilling Method (RDM). The RDM is a drilling technology particularly suited for long reach wells.

1.1 Background

Reelwell started a large Joint Industry Project called “ERD beyond 20 km” in 2011 (**Fig 1.1**). This project is supported by Shell, Total Petrobras and RWE Dea and the Research Council of Norway. The goal of the project is to verify the unique, extreme ERD capability, due to the following unique features:

- it enable flotation of the drill string, which can reduce torque and drag to a minimum,
- it enables screening out the dynamic ECD gradient,
- it provides means of hydraulic WOB, and
- it enables formation evaluation from cuttings – superior to conventional technology.

The field is located offshore in an environmentally very sensitive area. In order to avoid intrusion and minimize the risk of disturbing the sensitive environment, it may be required to develop this field by ERD from onshore to the offshore field.

Extended Reach Drilling, aiming to qualify and demonstrate drilling reach beyond 20 km. The main goal is to verify the RDM capability of safely and efficiently drilling ERD wells beyond the drilling reach of conventional drilling methods. Outstanding ERD performance is expected due to:

- Superior hole cleaning
- Significant reduction of torque and drag by buoyancy technique
- Improved downhole pressure and ECD control
- Reduced buckling including downhole traction

The Reelwell Drilling Method is a new unique concept of drilling. RDM uses a dual drillpipe, where one conduit is used for in-flow and the other conduit is used for return fluid from the well. **Fig 1.1** shows a schematic overview of the RDM arrangement vs, a conventional setup.

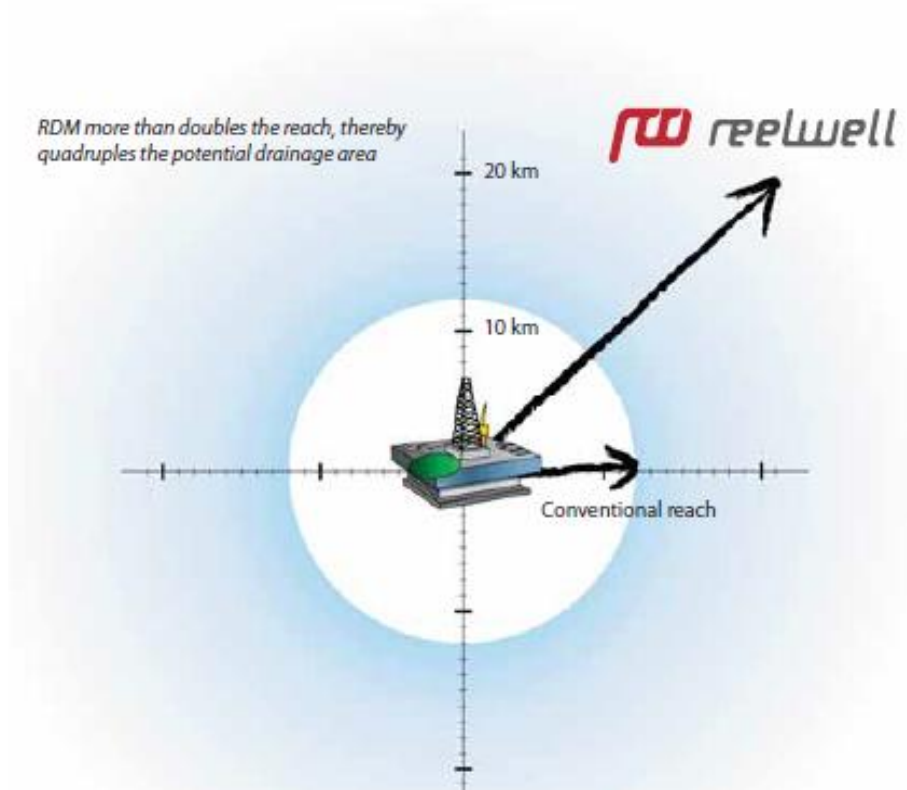


Fig 1.1 The RDM makes it possible to extend the horizontal reach. (Reelwell website)

1.2 Objective

The main objective with this thesis is to study the installation and cementation of a 10 3/4" casing and a 7" liner for Westertill prospect in Germany.

The main idea is to give an advice on how to do analysis and select operational safe parameters in order to:

- Install the casing and liner without problems regarding drill string mechanics.
- Cementing of the casing and the liner without fracturing the formation.

The activity of the thesis work includes:

- Simulation study with Landmark WELLPLAN.
- To perform sensitivity study with the reviewed and implemented hydraulics models in order to investigate the flow rate, fluid parameters and the length of cementing that can tolerate the fracture strength.

To limit the scope of the thesis, problems regarding burst and collapse of casing and drillpipe, and wellhead pressure will not be studied.

2 REELWELL Technology

2.1 Reelwell Drilling Method (RDM) vs. Conventional systems

The development of the Reelwell Drilling Method started in 2004 at Rogaland Research (today IRIS) in Stavanger. The RDM system has unique features for several applications like Extended Reach Drilling, Deep Water Drilling and Managed Pressure Drilling. Due to the hydraulic thrust force and unique hole cleaning, the RDM gives an opportunity to solve difficult challenges related to ERD. Reviewed

RDM differs from conventional drilling (Fig 2.1 in the circulation flow path of the drilling fluid. For conventional drilling the fluid returns up wellbore annulus, whereas in RDM the drilling fluid returns to surface through the inner pipe of the Dual Drill String (DDS). RDM is based on pumping the drilling fluid into the DDS annulus via the TDA and down to the DFV at the top of the conventional Bottom Hole Assembly (BHA). From the DFV the cuttings are transported back to surface inside the inner string, so that the hole remains clean at all times (Vestavik, Brown, & Kerr, 2009) .

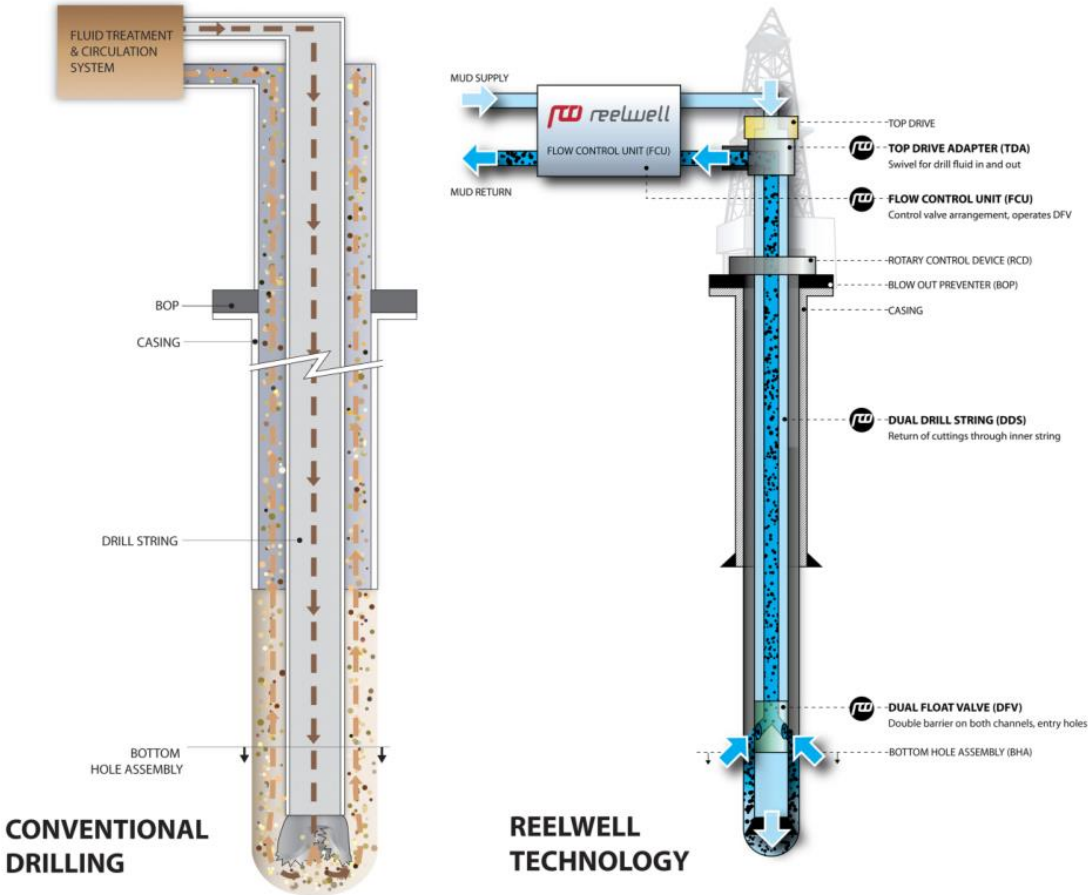


Fig. 2.1 Comparisons of conventional drilling and Reelwell technology

2.2 Components of the RDM system

Fig 2.2 is a schematic of the RDM system. The following components special tools and arrangements are used:

- The **Dual Drill String (DDS)** is a closed loop flow circulation system. Cuttings are transported to the surface by drilling fluid travelling up the central pipe of the dual string, leaving the wellbore annulus free of cuttings.
- The **Top Drive Adapter (TDA)** is a dual conduit swivel that allows rotation of the drill string with the top drive. The TDA route the discharge drilling fluid from the top drive to the DDS annulus and the return flow is taken of the TDA housing.

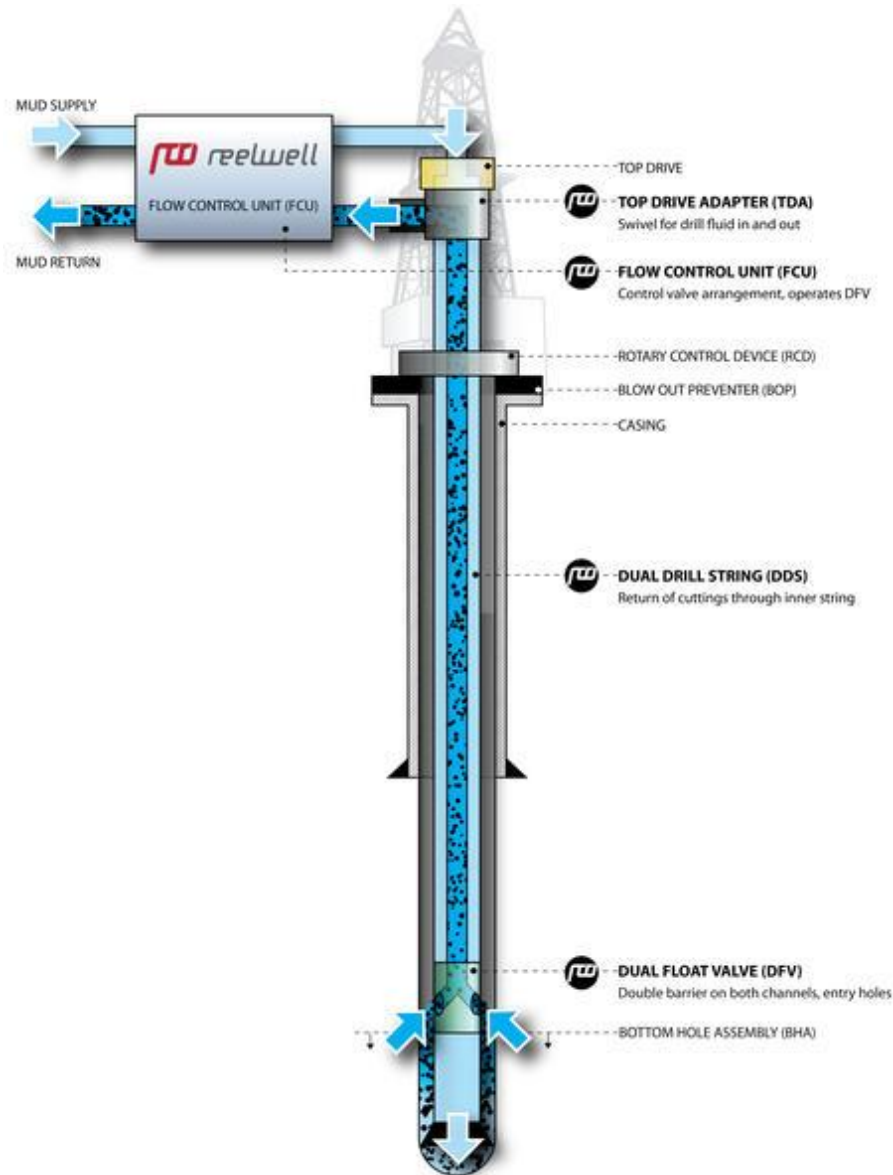


Fig 2.2 components of the RDM system

- The **Dual Float Valve (DFV)** contains double barriers on both channels and facilitates controlled pressure drilling and pressureless pipe connections. Two or more of the DFV can be mounted in series in the DDS for redundancy.
- The **Flow Control Unit (FCU)** is a control valve arrangement where all the active drilling fluid is routed through. The purpose is to assure constant downhole pressure during drilling and pipe connection. The unit is equipped with pressure and flow

sensors both on the drilling fluid inlet and return lines. The Reelwell control panel is fully integrated with the well control and monitoring system of the drilling facility.

In addition,

- an optional downhole piston may be attached to provide hydraulic WOB (pressure and force control) to increase the limit of horizontal reach. Conventional BHA can be used for directional drilling but MWD tools and motors may need adaption for reduced flow.
- Rotary Control Device (RCD): the RCD is placed on top of the BOP to ensure a proper seal during rotation of the drill string.
- An active circulating fluid (blue fluid in **Fig 2.3**) to power downhole tools and ensure proper hole cleaning,
- A passive high density well fluid (red fluid in **Fig 2.3**) to stabilize the hole and create the buoyance of the string. The passive fluid is trapped by the design of the RDM system.

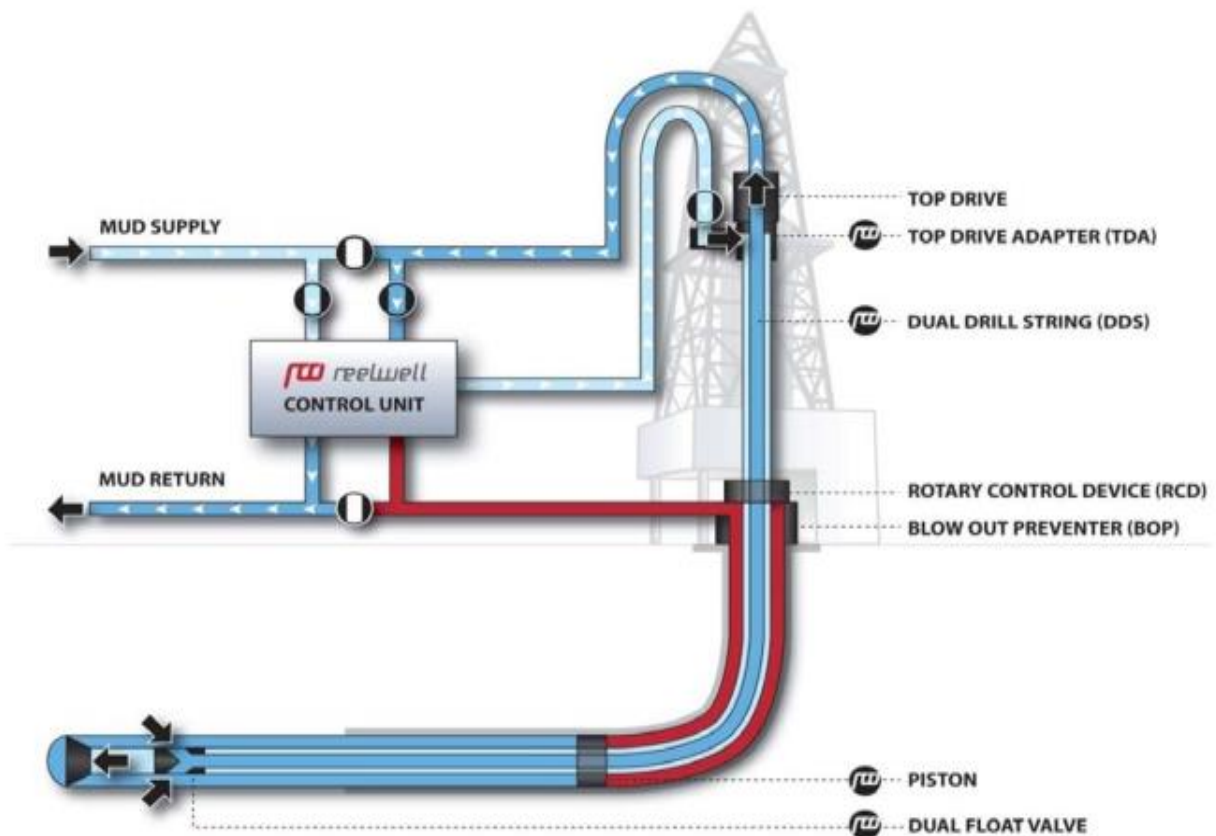


Fig 2.3 schematic of the equipment arrangement for the RDM (Belarde & Vestavik, 2011)

3 Literature study for simulation and installation procedure

This chapter presents the theory of the rheology models, pressure losses, ECD, and mechanics behind the simulation study in chapter 4. In addition, conventional installation procedure for 7” liner

3.1 Fluid rheology models

Azar and Robello Samuel define fluid rheology as: “Rheology is the study of the deformation of fluid. Its importance is recognized in the analysis of fluid flow velocity profiles, fluid viscosity, friction pressure losses, ECD, and annular hole cleaning. It is the basis for all analyses of wellbore hydraulics” (Azar & Samuel, 2007). **Fig 3.1** gives an illustration of typical behavior of different rheology models. One can see that each model gives a characteristic behavior when the fluid is applied a force. Note that the Power Law model is has a pseudoplastic behavior.

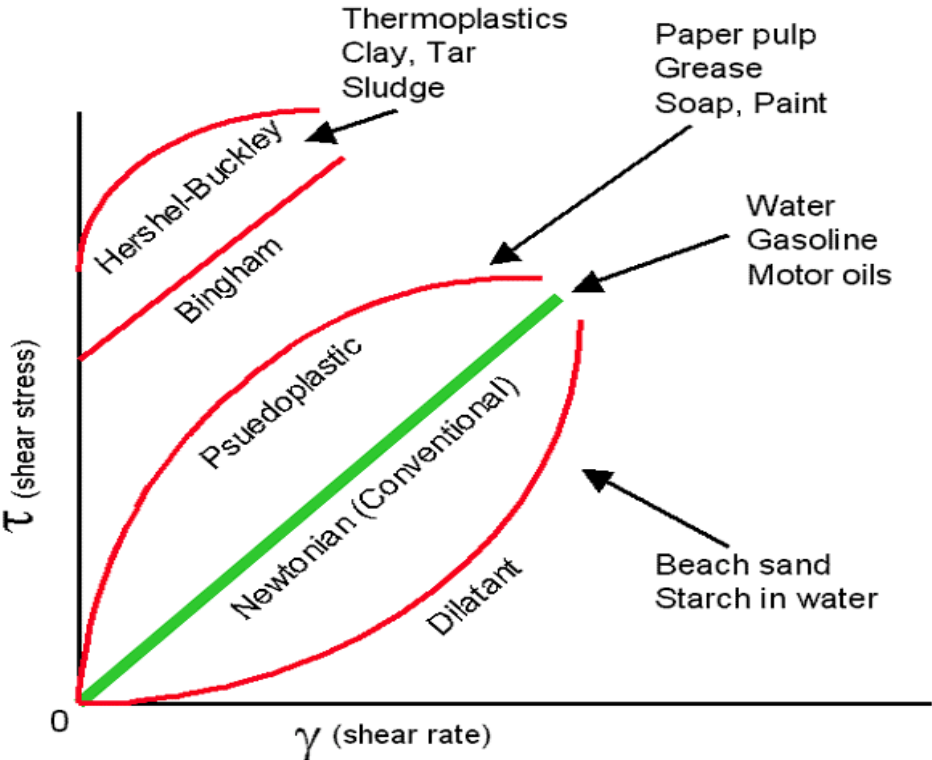


Fig 3.1 Illustration of rheology behavior (Pacific Northwest National Laboratory)

3.1.1 Bingham Plastic Model

The Bingham plastic model is a two-parameter model. However, it does not represent accurately the behavior of the drilling fluid at very low shear rates (in the annulus) or at very high shear rate (at the bit). The following equation gives the shear stress (τ) of the Bingham Plastic model (Bourgoyne, 1991)

$$\tau = \mu_p \gamma + \tau_y \tag{3.1}$$

Where μ_p is plastic viscosity, γ is shear rate and τ_y is the yield point

The yield point (τ_y) and plastic viscosity (μ_p) can be read from a graph or be calculated by the following equations

$$\mu_p (cP) = \theta_{600} - \theta_{300} \quad (3.2)$$

$$\tau_y \left(\frac{\text{lbf}}{1000\text{ft}^2} \right) = \theta_{300} - \mu_p \quad (3.3)$$

3.1.2 Power Law Model

The Bingham plastic model assumes a linear relationship between shear stress and shear rate. However, a better representation of the behavior of a drilling fluid is to consider a Power-law relationship between viscosity and shear rate. The shear stress (τ) of a Power Law Model is given as (Bourgoyne, 1991):

$$\tau = k\gamma^n \quad (3.4)$$

where k is the consistence index and n is flow behavior index.

An estimation of Power Law parameters can be made by the following equations:

$$n = 3.32 \log \frac{\vartheta_{600}}{\vartheta_{300}} \quad (3.5)$$

$$k \left(\frac{\text{lbf}\cdot\text{sec}^n}{100\text{ft}^2} \right) = \frac{\theta_{300}}{511^n} = \frac{\theta_{600}}{1022^n} \quad (3.6)$$

3.1.3 Herschel-Bulkley

The Herschel-Bulkley model defines a fluid by three-parameter. It's often preferred before Power-law or Bingham relationships because it results in more accurate models of rheological behavior. Mathematically it can be described by the following equation (Gucuyener, 1983):

$$\tau = \tau_0 + k\gamma^n, \text{ where} \quad (3.7)$$

$$\tau_0 = \frac{\tau^{*2} - \tau_{min}\tau_{max}}{2\tau^* - \tau_{min} - \tau_{max}} \quad (3.8)$$

Since this is a three-parameter model, an initial calculation of τ_0 is required for other parameter calculations. τ_0 is calculated as:

$$\gamma^* = \sqrt{\gamma_{min}\gamma_{max}} \quad (3.9)$$

where τ^* is the shear stress value corresponding to the geometric mean of the shear rate (γ^*)

3.2 Pressure losses

The downhole static pressures are easy to calculate from mud weight measured at the surface, while additional pressures caused by circulation can be calculated by using established relationships between pump rate and drilling fluid rheological properties.

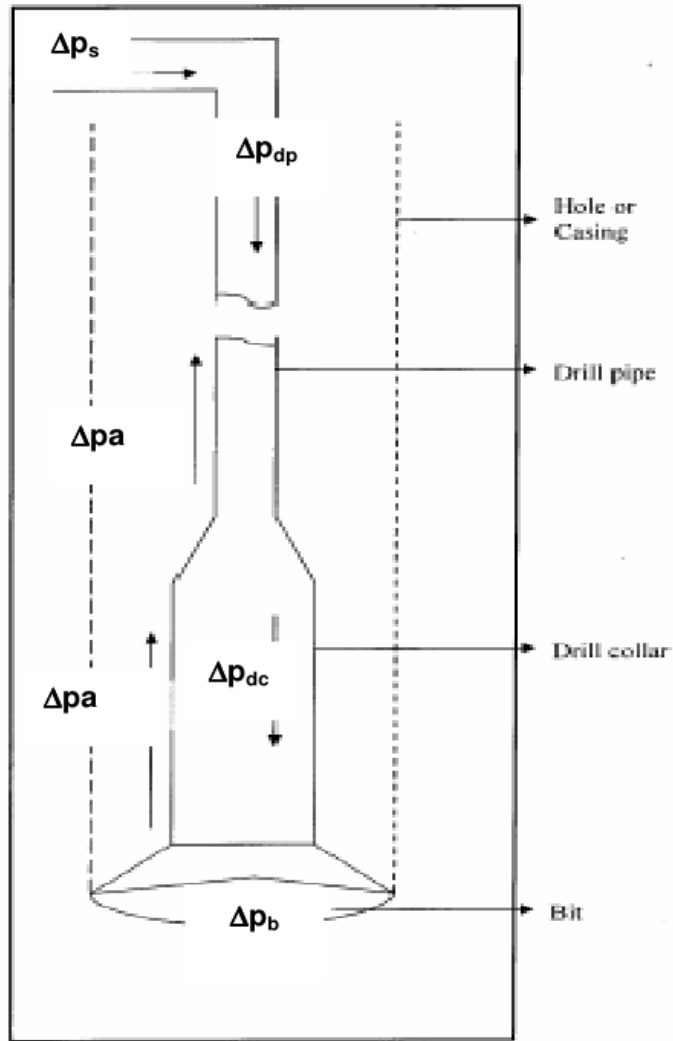


Fig 3.2 schematic of the pressure losses during circulation (H. Rabia, 1985)

During circulation of drilling fluid, friction between the drilling fluid and the wall of the drillpipe and annulus cause a pressure loss (**Fig 3.2**). Mathematically, the pump pressure loss (ΔP_p) can be expressed as:

$$\Delta P_p = \Delta P_s + \Delta P_{ds} + \Delta P_b + \Delta P_a \quad (3.10)$$

where ΔP_s is the frictional pressure loss in the surface equipment, ΔP_{ds} is the frictional pressure loss inside the drill string, ΔP_b is the frictional pressure loss across the bit and ΔP_a is the frictional pressure loss in the annulus.

3.2 Equivalent circulating density

During drilling or circulation, the friction pressure losses in the well will effectively increase the mud weight, resulting in an ECD (equivalent circulating density) that may cause fracture of formation. For a safe operation, the ECD must be higher than the fracture pressure. The ECD gradient is given as:

$$\rho^{ECD} = \rho + \frac{\Delta P_f}{gh} \quad (3.11)$$

where ρ is the wellbore fluid density, ΔP_f is the frictional pressure loss, g is the gravitational constant and h is the height of the fluid column. (Azar & Samuel, 2007)

3.3 Frictional pressure loss

An effective method to calculate the frictional pressure loss is to subdivide the drillstring and the annulus into shorter segments. This is important as a change in parameters like fluid density, flow regime or wellbore geometry is affecting the frictional pressure loss. (API, 2010).

Frictional pressure loss is a function of several factors such as:

- fluid parameters:
 - o Rheology behavior (Newtonian or non-Newtonian).
 - o Flow regime (laminar, turbulent or intermediate flow).
 - o Density.
 - o Viscosity.
 - o Flow rate.
- Drillstring configuration (tools, drill collar, etc.).
- Wellbore geometry (diameter, length, etc.).

The frictional pressure loss (ΔP_f) is mathematically given as:

$$\Delta P_f = \frac{2}{d_H} f_f \rho u^2 \Delta L \quad (3.12)$$

where d_H is hydraulic diameter, f_f is fanning friction factor, ρ is fluid density, u is fluid velocity, ΔL is segment length, q is volumetric flow rate, and A is cross-sectional area (Azar & Samuel, 2007).

The frictional pressure loss can be calculated as the following procedure:

1. Choose the best-fit rheological model and determine the rheological properties.
2. Calculate the Reynolds number by the correct formula based on the rheology model.
3. Decide the flow regime by compare the Reynolds number to the critical Reynolds number.
4. Calculated the friction factor, f by the correct formula based on the rheology model
5. Calculate the pressure loss by the correct formula based on the rheology model (Viloria, 2006).

3.3 Torque and drag

The torque and drag theory is the basis for the analysis of installation of liner and casing. This section reviews the theory behind the simulator.

3.3.1 Drag

The drill string mechanics module computes loads in drill string by tripping, and drilling condition. In addition to compute the buckling and tensile load limits. The main objective is to describe the allowable loads on drill string, which is bounded by the buckling and the tensile limits.

The physics behind the torque and drag model is obtained by force balance. When calculating buckling loads and torque & drag forces, all loads must be computed with respect to a given well geometry (inclination, azimuth and MD). The drill string is assumed to be divided up into a number of short jointed segments (cells) through which the transmission of tension, compression and torsion are allowed.

Fig 3.3 shows a simple free-body diagram of a drill string segment with respective loads.

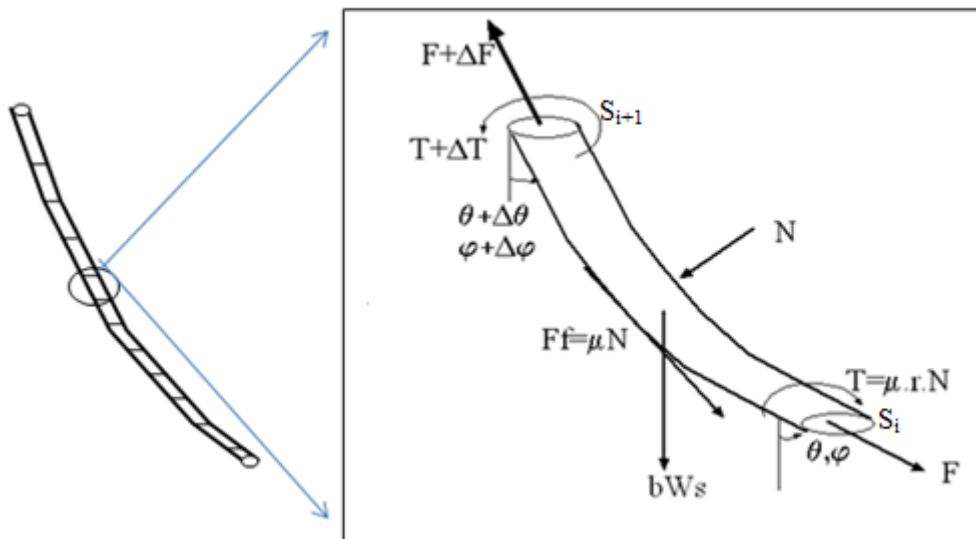


Fig 3.3 schematic of a segmented drill string

Applying the condition of equilibrium along the axial and normal directions, the effective force along the axial direction is (Aadnoy, Fazelizadeh, & Hareland, 2010):

$$\frac{dF}{ds} = \pm \mu_a N + \beta w_s \cos \theta + \frac{dF_{fl}}{ds} \quad (3.13)$$

Johancsik et. al. (1984) derived the normal force per unit length in any curved well geometry that shows variation in inclination and azimuth (Johancsik, Friesen, & Dawson, 1984):

$$N_i = \sqrt{\left(\beta w_{si} \sin\left(\frac{\theta_{i+1} + \theta_i}{2}\right) - F_i \left(\frac{\theta_{i+1} - \theta_i}{S_{i+1} + S_i}\right)\right)^2 + \left(F_i \sin\left(\frac{\theta_{i+1} + \theta_i}{2}\right) - F_i \left(\frac{\varphi_{i+1} - \varphi_i}{S_{i+1} + S_i}\right)\right)^2} \quad (3.14)$$

When drilling at various angular rotational speeds and when tripping in/out, the drillstring is at various axial speeds. These dynamic parameters affect the axial and tangential friction coefficients, and will be considered in the torque and drag model as the following (Aadnoy et al., 2010):

The axial friction factor:

$$\mu_a = \mu \sin \alpha \quad (3.15)$$

Where the angle α is given by: $\tan \alpha = \frac{v_a}{r\Omega}$. r is the drill string radius, Ω is the angular velocity of rotation and v_a is the axial speed. v_a is defined positive for tripping in and drilling, and negative for pulling out:

$$F_{i+1} = F_i + \sum_{i=1}^n \left[\beta w_i \cos\left(\frac{\theta_{i+1} + \theta_i}{2}\right) \pm \mu_t N_i \right] (S_{i+1} - S_i) \quad (3.16)$$

$F_{a(i)}$ is the bottom weight when integrating from bottom to top. The positive sign is for run out of the hole and the negative sign is run into the hole.

3.3.2 Torque model

The torque for both buckled and non-buckled string is given as:

$$T_{i+1} = T_i + \sum_{i=1}^n \mu_t r_i N_i (S_{i+1} - S_i) \quad (3.17)$$

where the tangential friction factor, $\mu_t = \mu \cos \alpha$, is always positive. N_i is the contact force per unit length.

3.4 Running and cementing of liner

3.4.1 Conventional running and cementing of liner

A liner is assembled joint-by-joint at the rotary table and lowered into the well. Depending on if rotation is planned during cementing, premium connections to withstand high torque are required. **Fig 3.4** shows a schematic of the liner setting tool and hanger assembly. The

purpose of the float shoe is to direct the casing smoothly into the hole, minimize well-side cavings and ensure a safe passing through crooked holes. The landing collar is to provide a seat for the liner wiper plug. Centralizer must be installed at a given length to keep the liner clear of the borehole wall. A centralized liner will improve the fluid displacement significantly.

The liner is run into the well using drillpipes with a special setting tool. The liner-setting tool is actuated so that the liner is attached mechanically to and supported by the casing without hydraulically sealing the passage between the liner and the casing. The cement slurry is pumped down the drillpipe, while a latch-down plug behind the cement slurry is separating it from the displacement fluid. The latch-down plug actuates a special wiper plug in liner-setting tool after the top of the cement column reaches the liner. Then the wiper plug reaches the float collar, an increase in pressure at the surface signifies the end of the cement displacement job. The drillstring then must be released from the liner-setting tool and withdrawn before the cement hardens. Normally, a cement volume sufficient to extend past the top of the liner is displaced. This cement can either be washed or drilled out after the cement is hardened.

There is a large variety of different liner-setting tools. Most of the liner-setting tools are set with either a mechanical or hydraulic devices. The hydraulically set devices are actuated by drillpipe rotation or by dropping a ball/plug and then set by applying pump pressure. The mechanically set devices are actuated by drillpipe rotation and set by lowering the drillpipe. A proper liner-setting tool must be selected on the basis of the liner weight, cement displacement rate, annular dimensions and liner-cementing procedure. Lately, several cementing jobs have been performed where the liner is not set until after the cement displacement. This allows the liner to be moved during cementing displacement to improve the mud removal in the annulus. This practice imposes some limitations on the selection of conventional liner-setting tool. However, expandable liner hangers can be moved easily while cementing and may lower cement placement pressures by having a larger cross sectional flow area in the liner lap (Nelson & Guillot, 2006) (Mitchell & Miska, 2011).

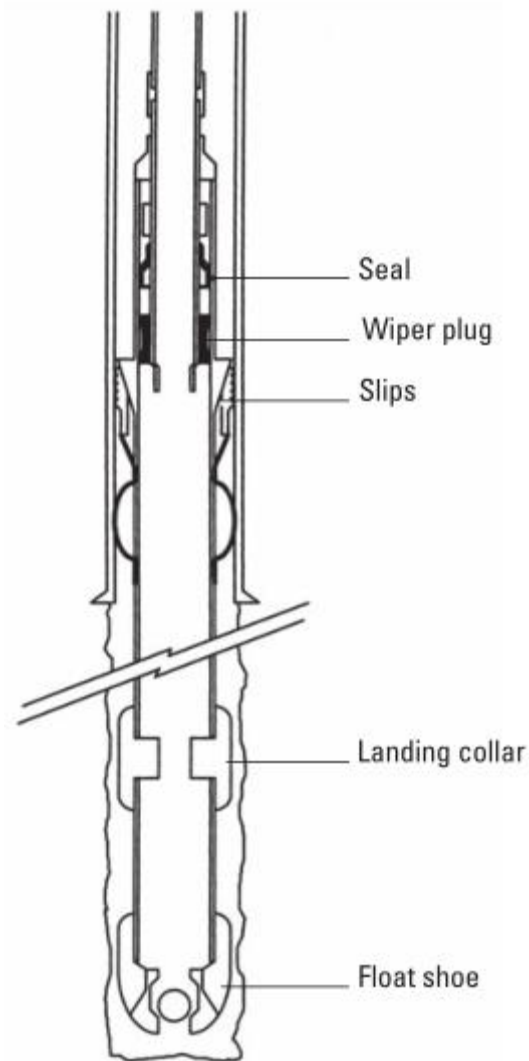


Fig 3.4 schematic of liner setting tool and hanger assembly(Nelson & Guillot, 2006)

3.4.2 Field Case study – Visund Field in the North Sea

The 34/8-A-6 AHT2 well in the Visund Field has a Measured Depth of 9,082 m and an Along Hole Depth of 7,593 m. The following casing or liners was installed:

- 30" conductor
- 20" casing,
- 13 ³/₈" casing,
- 10 ³/₄" liner, and
- 7" liner.

Data for the 10 ³/₄" liner and the 7" liner is given in **Table 3.1** and **Table 3.2**.

10 ³/₄" liner installation

By controlling the friction factor, the liner could be run conventionally without buckling the string. The control of the friction factor was extremely important, and three other Visund well

above 7,000 m measured depth were analyzed and calibrated for friction factors. Based on the friction factors for cased hole and open hole the liner running string was designed to withstand helical buckling. The liner was designed with a convertible open liner shoe to allow the liner to be filled when running into the hole, and thus, lower the surge pressures.

The liner was easily ran into the whole, but the frictional was hugely increased for the last 600 m of the open hole section. The running procedure was stopped 150 m above the bottom of the well. However, this setting depth was acceptable for further drilling, and the liner was set and cemented.

Table 3. 1 liner data

Outer Diameter	10 ¾"
Length	4,600 m
Open Hole section	2,820 – 7,415 m (4,595 m)

7" liner installation

Table 3. 2 liner data

Outer Diameter	7
Length	1,885 m
Open Hole section	7,265 – 9,082 m (4,595 m)

The liner was run into the well without any problems by friction. The med weights was reduced was reduced prior to the cementing operation to reduce the ECD. The 7" liner was cemented with a flow rate of 1,500 l/min with no loss of fluids. The only problem with the cementing was that the top wiper plug was set too early, leaving 480 m of cement insider the 7" liner. However, this was not a problem as it was enough excess cement to cement the whole length of the annulus between the liner and the wellbore wall.

Experiences from the field show that:

- Optimum well profile is important to reduce the friction factor, and thus, reduce the torque.
- A good friction factor calibration is critical to achieve a safe operation.
- Successful control of surge pressures due to the convertible open liner shoe.
- It is possible to drill and complete even longer wells, with an optimal preplanning in cooperation with the service companies. 3D visualization and simulation tools are important for the preplanning (Hjelle et al., 2006).

4 Simulation study using Landmark WELLPLAN

The simulations in this chapter are simulated with Landmark WELLPLAN 5000.1. The following WELLPLAN modules are used for the simulations:

- Torque Drag – Normal Analysis module to simulate the installation, and
- OptiCem-Cementing – Wellbore Simulator to simulate the cementing operation.

4.1 Simulation study installation and cementation of 10 3/4” casing

The main objective of this section is to show how the installation of the 10 3/4” casing is possible; with respect to drill string mechanics to make sure that the drag is within the operational limits (buckling and tensile). The torque is not evaluated in the simulation as the WELLPLAN software gave results which could be seen as untrustworthy.

During simulation various operation parameters are evaluated. These parameters are RPM, running speed, and coefficient of friction.

4.1.1 Simulation of 10 3/4” casing installation

4.1.1.1 Simulation arrangement

Table 4.1 show the hole section for the well. The previous set casing is a 13 3/8” casing with the casing shoe at 5,000 m MD. The open hole section is from 5,000 – 14,000 m MD.

Table 4.2 shows drill string arrangement for the 10 3/4” casing. As the casing is reaching from the bottom of the well to the surface, the drill string is consisting only of a 14,000 m section of 10 3/4” casing. Geometry, nominal weight, grading and connection are also listed in the table.

Table 4.3 gives other data for the simulation.

Fig 4.1 illustrates a schematic of the well including the drill string arrangement.

Fig 4.2 illustrates the vertical section of the well.

Table 4. 1. Hole section on

Section Type	MD [m]	Length [m]	ID [in]	Drift [in]	Effective Hole Diameter [in]	Item Description
Casing	5,000	5,000	12.61	12.459	12.715	13 3/8 in, 54.5 ppf, M-65
Open Hole	14,000	9,000	12.15		12.25	

Table 4. 2. Drill string arrangement

Section Type	Length [m]	OD [in]	ID [in]	Item Description
Casing	14,000	10.75	9.85	10 3/4 in, 51 ppf, N-80

Table 4. 3. Parameters for the simulation

Parameter:	Value:
Pump flow rate	500 l/min
Mud density	1.55 s.g.

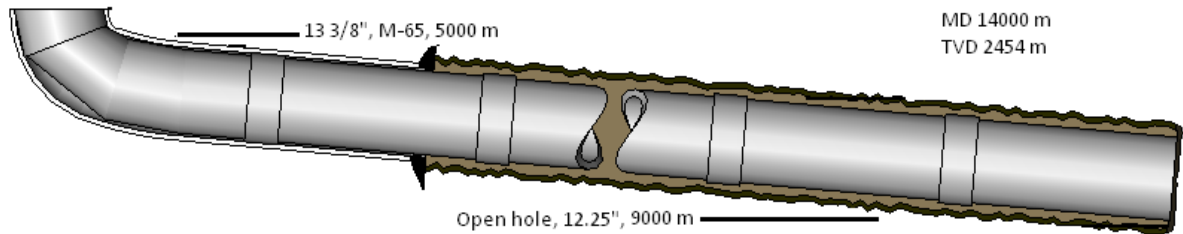


Fig 4.1 Schematic of hole section and drill string arrangement

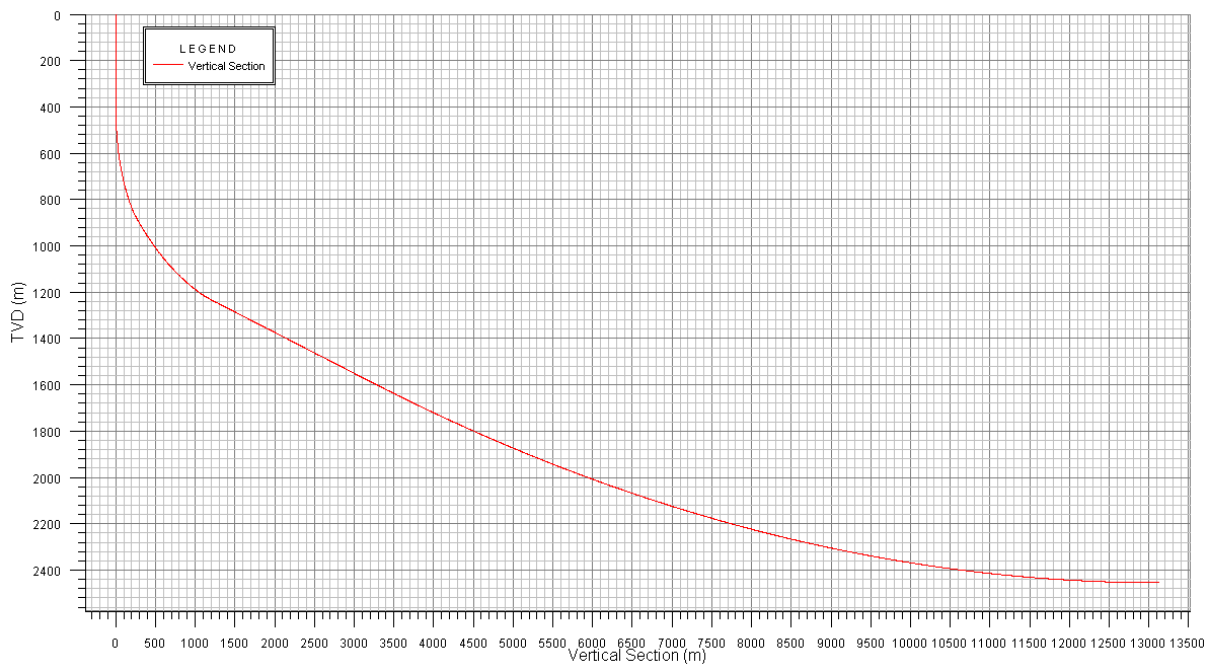


Fig 4.2 Vertical section of the well

4.1.1.2 Simulation result

The following three simulations show that, without any rotation, the casing can be tripping out without breaking it by tension. However, a rotation of the string must be applied when tripping in. The maximum running speed for tripping in or tripping out is a function RPM and friction coefficient. The maximum running speed for tripping in or tripping out is a function of these two operational parameters (Aadnoy et al., 2010).

Simulation #1.1

The tripping in/out speed and friction factor is given in **Table 4.4**. At this speed, the whole 14,000 m string can be tripped in or tripped out by 25.5 hours. This is quite a long time and will give a high cost to the company.

Fig 4.3 gives the tension for tripping in/out for three different RPM. The tripping in 0 RPM curve shows that it will buckle sinusoidal as the curve is crossing the sinusoidal buckling limit. The string will not break by tension for any RPM, as none of the curves are crossing the tension limit.

Fig 4.3 shows that the limit for sinusoidal buckling is 20 RPM at tripping in. A third simulation of 60 RPM can also be seen from the figure. The tendency is that when the RPM is increased, the tripping in tension will increase, while the tripping out tension will decrease. This is due to an increase of RPM is changing the axial friction according to **Eq. (3.15)**. Aadnoy et. al. (2010) shows that when the running speed is doubled, the angular speed (RPM) must also be doubled. This has a similarity to if you put a stick down in the ground. It can be hard to pull it up from the ground, but if you rotated the stick, this will be much easier. However, be aware of the increase of torque when the RPM is increased.

Table 4.4. Simulation parameters

Parameter:	Value:
Friction factor Cased Hole	0.20
Friction factor Open Hole	0.30
Tripping In/Out speed	30 ft/min

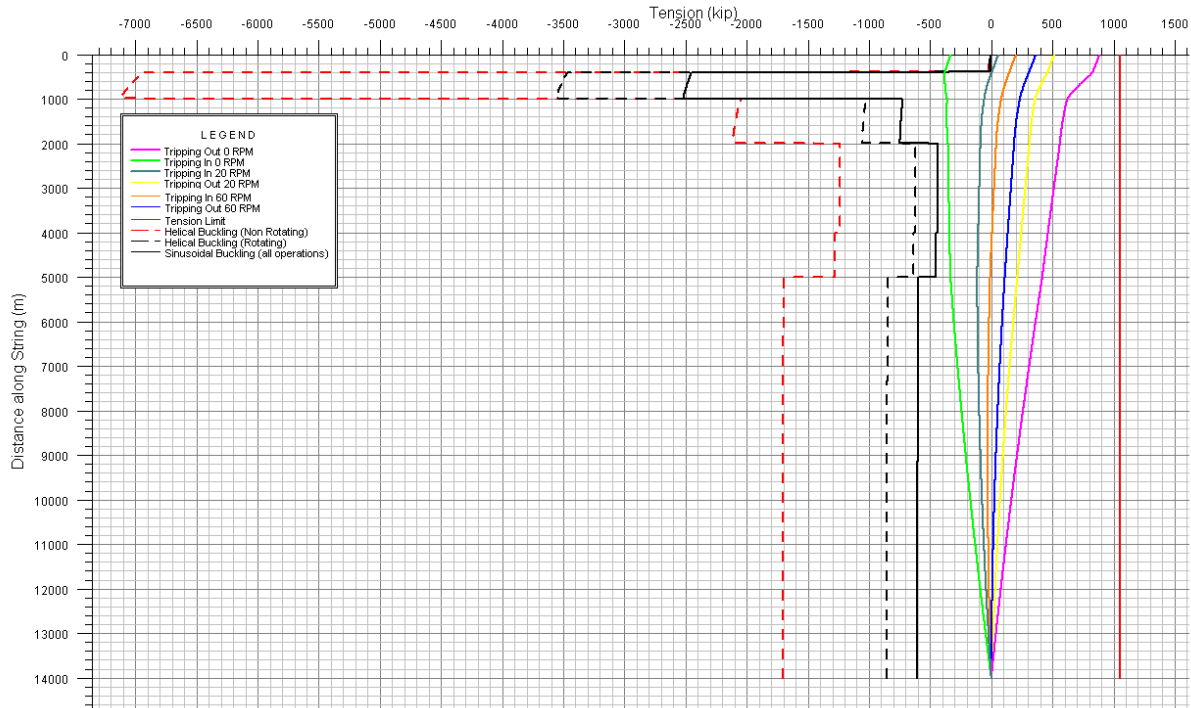


Fig 4.3 Effective tension by tripping in/out for various RPM

Fig. 4.3 shows that it is possible to avoid tension and buckling by increasing the RPM. Due to the length of the well, a high trip in and trip out speed is preferred to reduce the time. This leads to Simulation #1.2, where the running speed is increased.

Simulation #1.2

The tripping in/out speed and friction factor is given by **Table 4.5**.

Fig 4.4 gives the tension for tripping in and tripping out for three different RPM. Note that the tripping in 0 RPM curve and tripping put 0 RPM curve is the same as for Simulation #1.1 for 0 RPM (**Fig 4.3**). **Eq. (3.15)** shows that the tension is independent of the running speed when there is no rotation of the string.

Table 4.5. Simulation parameters

Parameter:	Value:
Friction factor Cased Hole	0.20
Friction factor Open Hole	0.30
Tripping In/Out Speed	60 ft/min

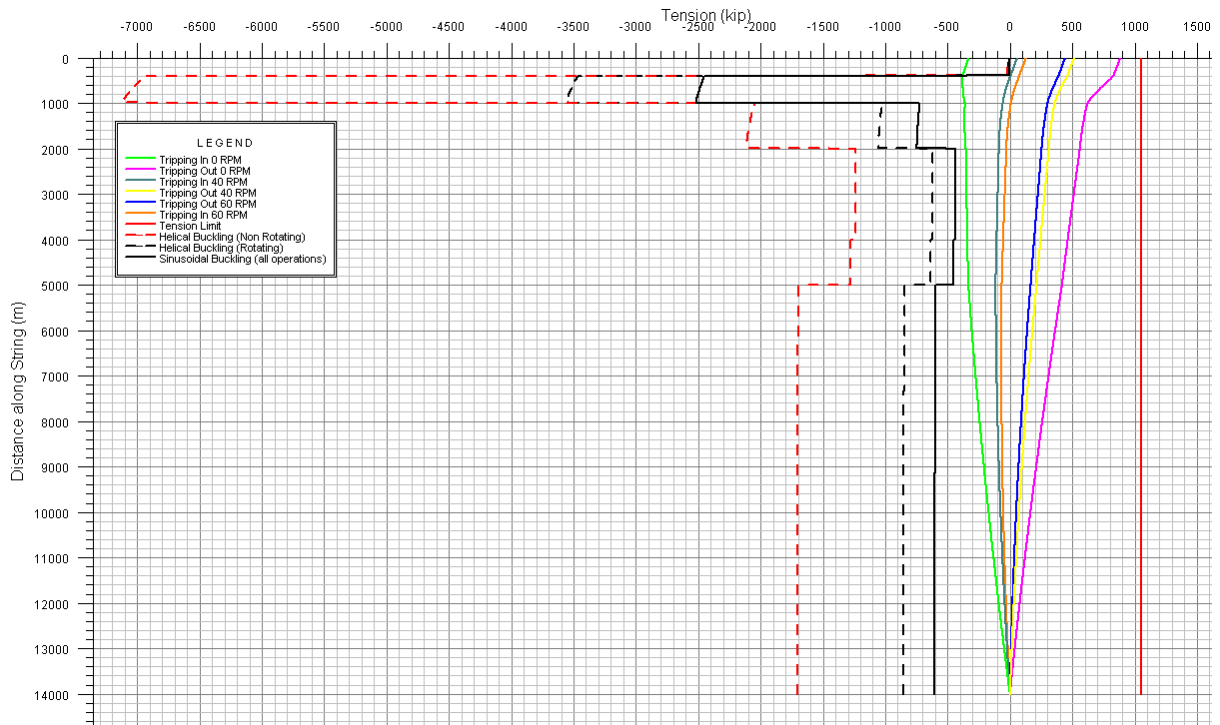


Fig 4.4 Effective tension by tripping in/out for various RPM

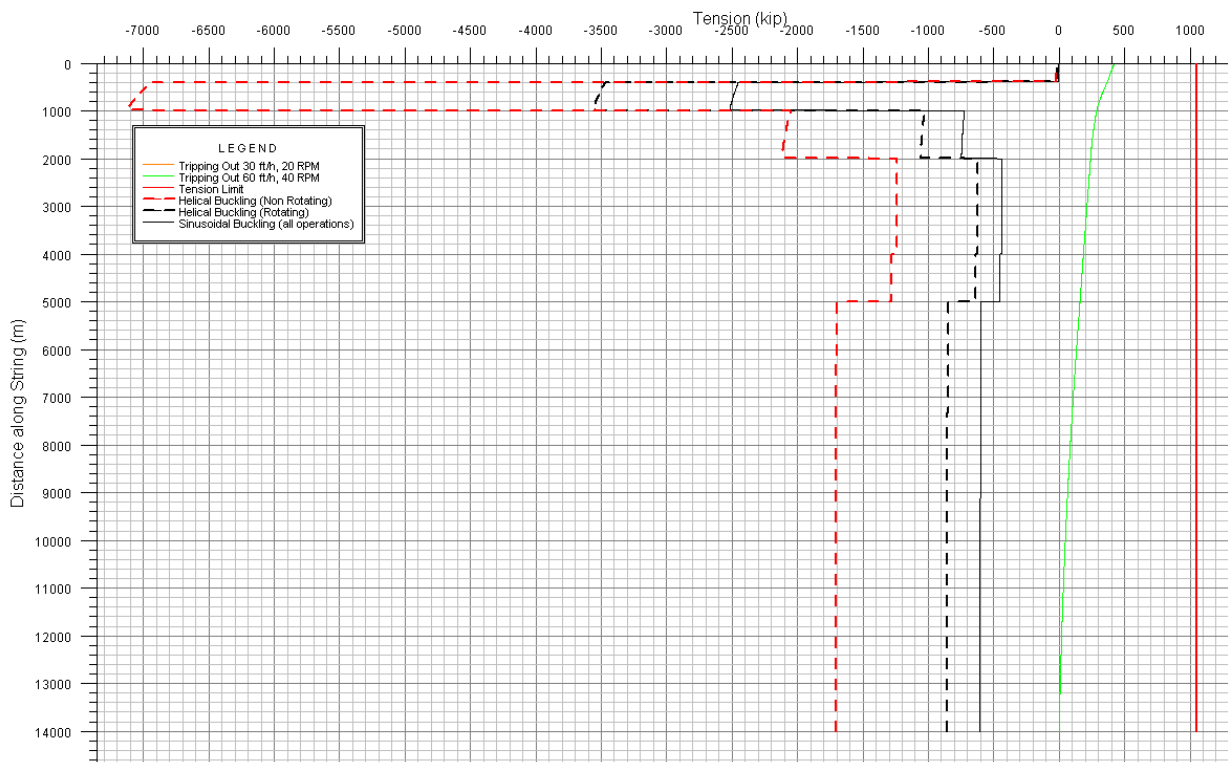


Fig 4.5 Effective tension for 20 RPM and 40 RPM

Fig 4.4 shows that the string must be rotated by 40 RPM to avoid Sinusoidal Buckling by tripping in. For Simulation #1.1, the RPM to avoid Sinusoidal Buckling was 20 RPM. From

Fig 4.5 one can see that when the speed is doubled, the RPM also must be doubled to achieve the same tension vs. distance along the string. This is according to theory of drag (Aadnoy et al., 2010) and can be seen from **Eq. (3.15)**. Note that the yellow curve cannot be seen from the figure as it is exactly the same as the green curve (hidden behind the green curve).

It's seen that an increase of RPM is decreasing the friction between the drill string and the wellbore. The friction can also be reduced by reducing the friction factor of the casing and the open hole. This leads to simulation #1.3.

Simulation #1.3:

Fig 4.6 shows the tension curve for 60 ft/min and 60 RPM while the friction factor is changed for three different cases according to **Table 4.6**. The friction factor can be change by adding a friction reducing agent to the well fluid (White, 1964) (Chen, Fu, Rey, Kouba, & Fouchi, 2000). The figure show that and decrease of the friction factor will reduce the tension by tripping out and increase the tension by tripping in. This is as expected as an increase of the friction will make it more difficult to move the string.

Table 4. 6 Simulation parameters

	Parameter:	Value:
	Tripping In speed	60 ft/min
	Tripping Out speed	60 ft/min
	RPM Tripping In	60 RPM
	RPM Tripping Out	60 RPM
Case 1:	Friction factor Cased Hole	0.20
	Friction factor Open Hole	0.30
Case 2:	Friction factor Cased Hole	0.15
	Friction factor Open Hole	0.25
Case 3:	Friction factor Cased Hole	0.10
	Friction factor Open Hole	0.20

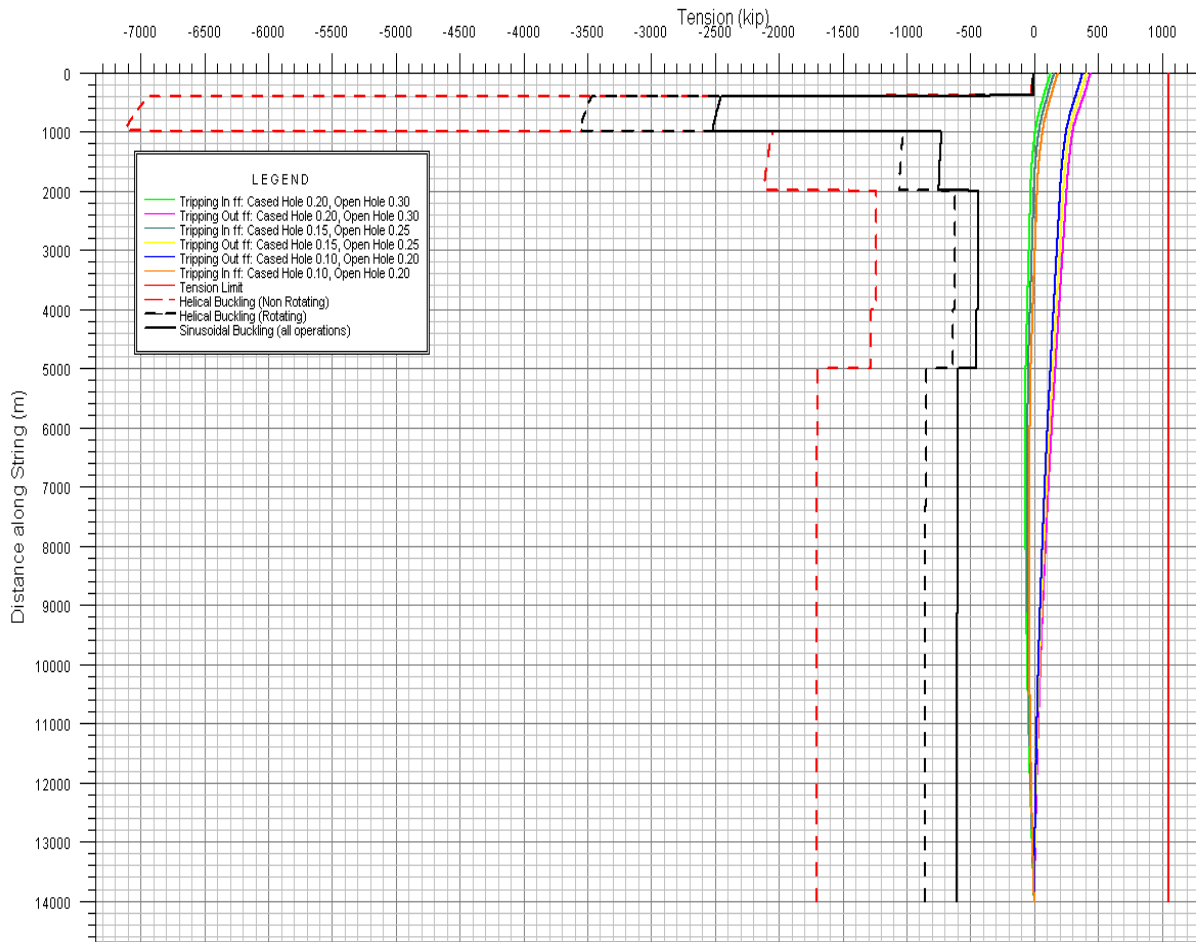


Fig 4.6 Effective tension for various friction factors

4.1.2 Simulation of cementation 10 3/4" casing

4.1.2.1 Simulation arrangement

Table 4.7 gives important data such as rheology and density for the mud, spacer and cement.

Fig 4.7 shows the pore and fracture pressure vs. MD for the well. Note that the figure gives what the actual pressure is in bar, and not the gradient. The figure also gives the information of the pore pressure gradient and fracture pressure gradient.

Table 4.8 show how the cement job is planned. In the first stage of the operation, the well is circulated with mud. Then 20 bbl. of spacer is entered the well, followed by a cement volume which equals to a length of 9,000 m in the annulus. Then the Top Plug is entering the well, followed by the same mud as in the first stage. The rate is set to a constant of 1,000 l/min in this example.

Fig 4.8 shows an illustration of how the cement is displaced and set in the annulus between the casing and the wellbore wall. The top figure is when the cement is pumped downwards inside the 10 3/4" casing. Bottom figure is at the end of the cement job The circulating is stopped to let the cement set and harden

Table 4.7 Data for cementing fluids

Mud		Spacer		Cement	
Density [s.g.]		Density [s.g.]		Density [s.g.]	
1.55		1.57		1.60	
Rheology Model		Rheology Model		Rheology Model	
Generalized Herschel-Bulkley		Generalized Herschel-Bulkley		Generalized Herschel-Bulkley	
Mud base type				Yield [ft ³ /sk]	
Oil				1.18	
				Water reg. [gal/sk94]	
				5.50	
Fann Data:		Fann Data:		Fann Data:	
Speed [RPM]	Dial [°]	Speed [RPM]	Dial [°]	Speed [RPM]:	Dial [°]
600	57	300	59	300	76
300	50	200	49.5	200	56
200	37	100	37.5	100	39
100	24	60	31.5	60	31
6	7	30	26.5	30	25.5
3	6	6	19	6	19
		3	18.5	3	17

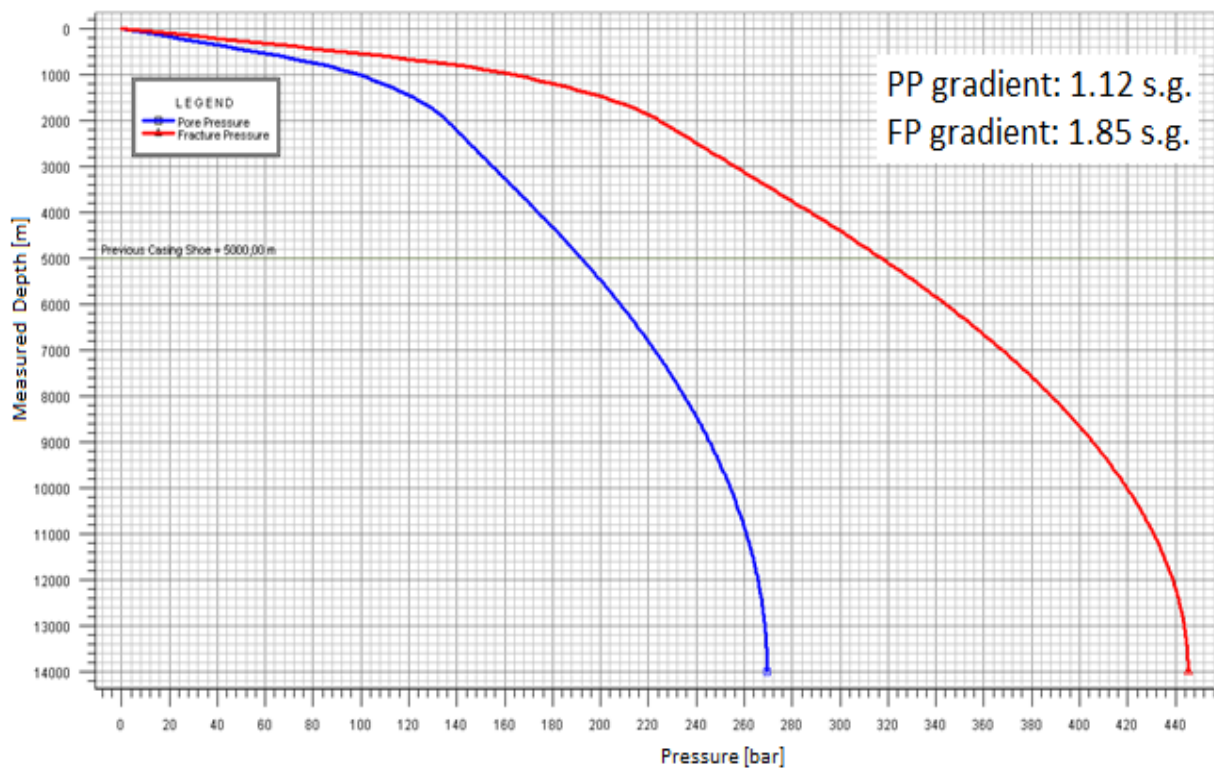


Fig 4.7 Pore and Fracture pressure

Table 4. 8. Cementing data from WELLPLAN/OptiCem

Stage No	Fluid	Density (s.g.)	Placement Method	Rate [l/min]	Length [m]	Duration [min]	Volume [bbl]
1	Mud	1.55	Volume	1000	4588.99	-	-
2	Spacer	1.57	Volume	1000	144.01	3.18	20
3	Cement	1.60	Length	1000	9000	157.82	992.68
4	Mud	1.57	Volume	1000	13990	687.78	4325.99

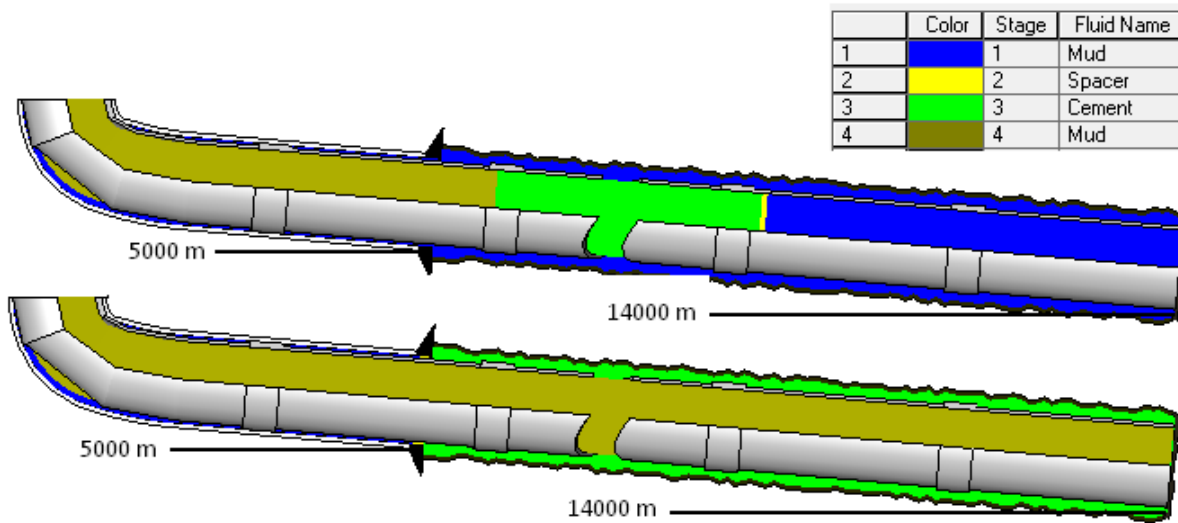


Fig 4.8 Schematic figure of the cementing job

4.1.2.2 Simulation result

The following five simulations show that the cementing job can be done by changing the operation parameters. The density and rheology of the cementing fluids, and the flow rate has a great influence on the frictional pressure loss. If these parameters have reached its operational limits, the length of the cemented section can be reduced. Note that this will not change the ΔL from Eq. (3.12), but will reduce the overall average density and rheology of the combined cementing fluids, as the cement is denser and more viscous than mud.

Simulation #2.1:

In this simulation, the cemented length is set to 9,000 m (from 14,000 – 5,000 m MD) and the flow rate is set to 1,000 l/min (see Table 4.9). Fig 4.9 shows the maximum ECD vs. MD during the complete cement operation, which includes pumping the cement down the casing and back up the annulus. As the figure show, Maximum ECD curve is crossing the Fracture Gradient at 3,000 m. The well is protected by casing from the surface to 5,000 m MD and it will withstand the pressure. However, one must expect that the fracture may propogate from the open hole section at the casing shoe to the formation behind the casing. Note that the steepnes of the curve in Fig 4.9 is changing at the casing shoe at 5,000 m. The reason for this is that the wellbore geometry is changed at this point. The annulus is tighter below this point, which will increase the pressure loss below this point.

The ECD is a function of the TVD and frictional pressure loss. The highest ECD must be at the bottom of the well as this is the deepest point of the well (can be seen from **Fig. 4.2**), and the frictional pressure loss has its highest value, as the frictional pressure is a function of length (**Eq. 3.11**). **Fig 4.9** show that the ECD is highest at the bottom of the well. The ECD will have its greatest value at the bottom of the well at the end of the cementing operation, when the hydrostatic fluid column consist of 9,000 m cement and has the greatest ratio of cement vs. mud/spacer). The cement is more dense and has greater viscosity than the mud and spacer. The frictional pressure loss is a function of density and viscosity and will increase if there is an increase of density and/or viscosity.

As the well is fractured in this simulation, some parameters must be changed. This lead to **Simulation #2.2**, where the flow rates is reduced to see if the cementation can be done without fracturing the formation

Table 4.9 Simulation parameters

Parameter	Value
Cemented length	9,000 m
Flow rate	1,000 l/min

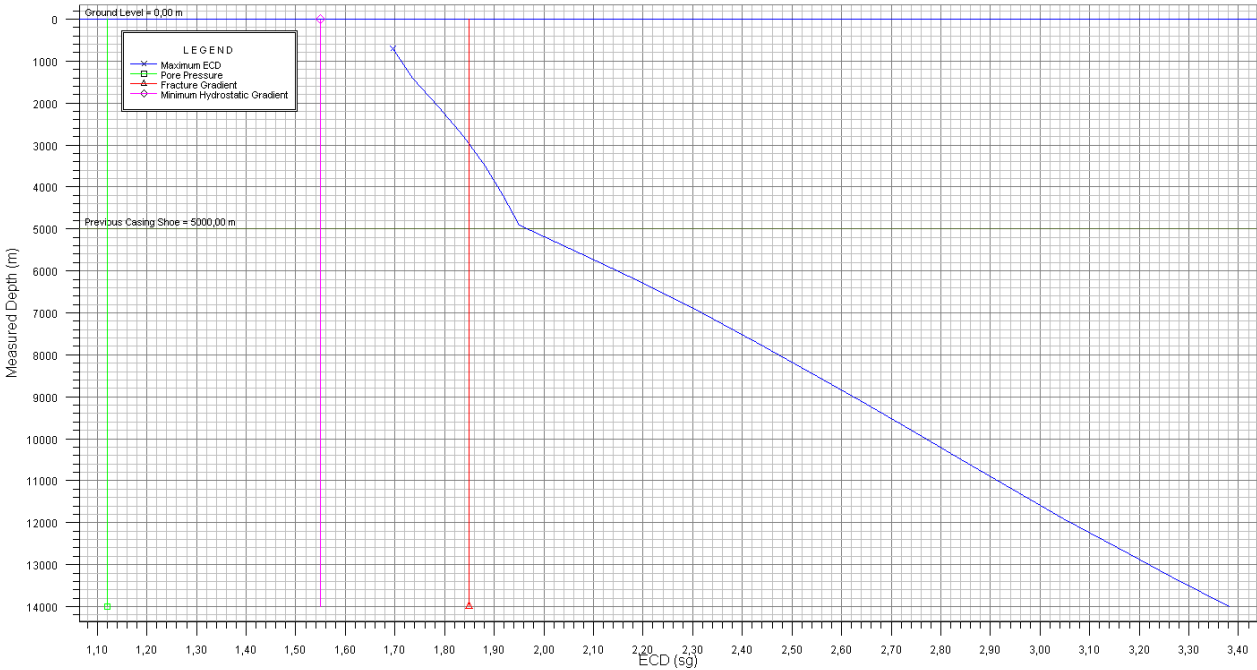


Fig 4.9 Maximum downhole pressure profile for the cement job for displacement at 1,000 l/min

Simulation #2.2

Table 4.10 gives the flow rate for this simulation. The cemented length is still 9,000 m. A reduction of the flow rate will surely increase the time to perform the cementing operation. The time duration from when the cement is entering the well to it is placed behind the casing and circulation is stopped, is given in the same table. A flow rate as low as 100 l/min should

be avoided as it would be very costly to the company due to the time of the cementing operation.

Fig 4.10 shows the maximum ECD for different flow rates. The figure show that the formation will fracture even at a flow rate of 100 l/min.

To check if the ECD is greatly affected by the length of the well, a simulation where the measured length is reduced is done in **Simulation #2.3**.

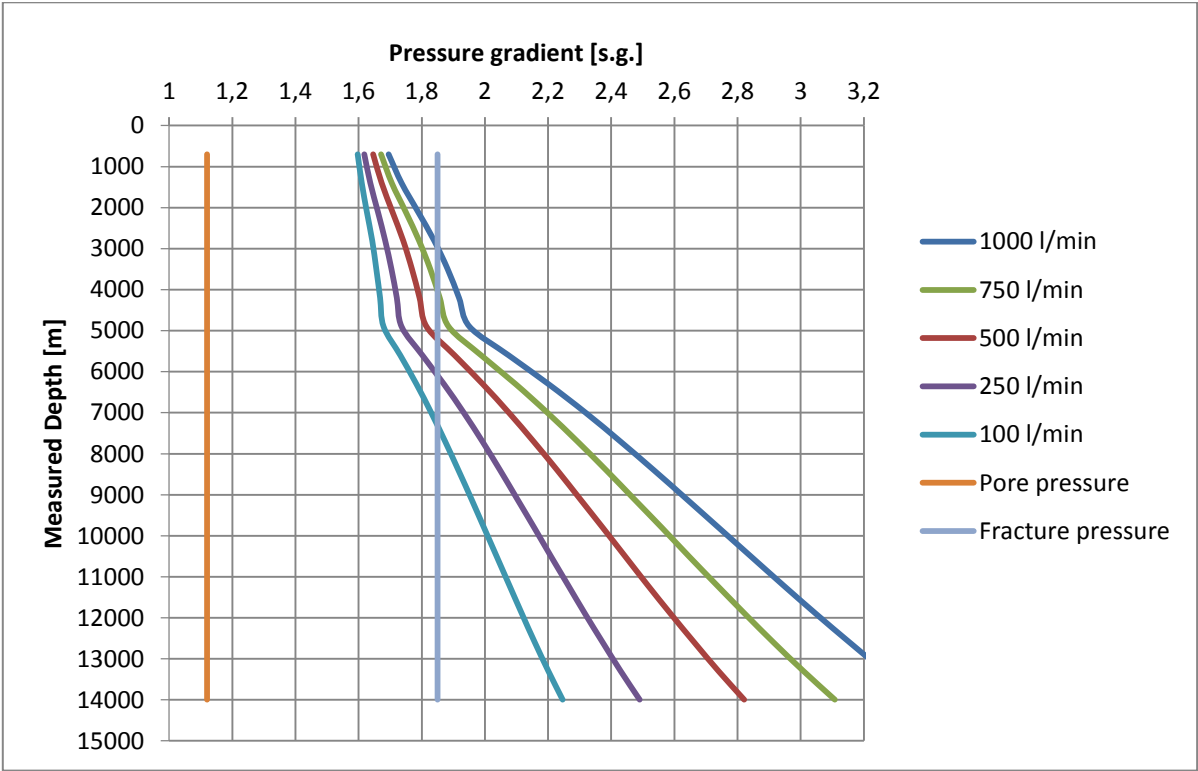


Fig 4.10 Maximum ECD for various flow rates

Table 4. 10. Displacement time for various flow rates

Flow rate [l/min]:	Duration [hours]:
1000	14.1
750	18.9
500	28.3
250	56.6
100	141.5

Simulation #2.3

The measured depth is decreased from 14,000 m to 8,000 m to see how this will affect the ECD (by reducing the length and thus the frictional pressure loss). The cemented length is still 9,000. **Fig 4.11** shows the Maximum ECD at a flow rate of 100 l/min where it is assumed

that the drilling was stopped at 8,000 m MD. Note that the TVD is not the same as in **Simulation #1.1** or **Simulation #2.2**, as this simulation was more of a sensitivity analysis.

The ECD is reduced in this simulation compared to Simulation #2.2, but the formation will fracture even at this low flow rate of 100 l/min. As the pressure loss is a function of rheology and density of the fluid, these parameters must be evaluated. This is done in Simulation #2.4.

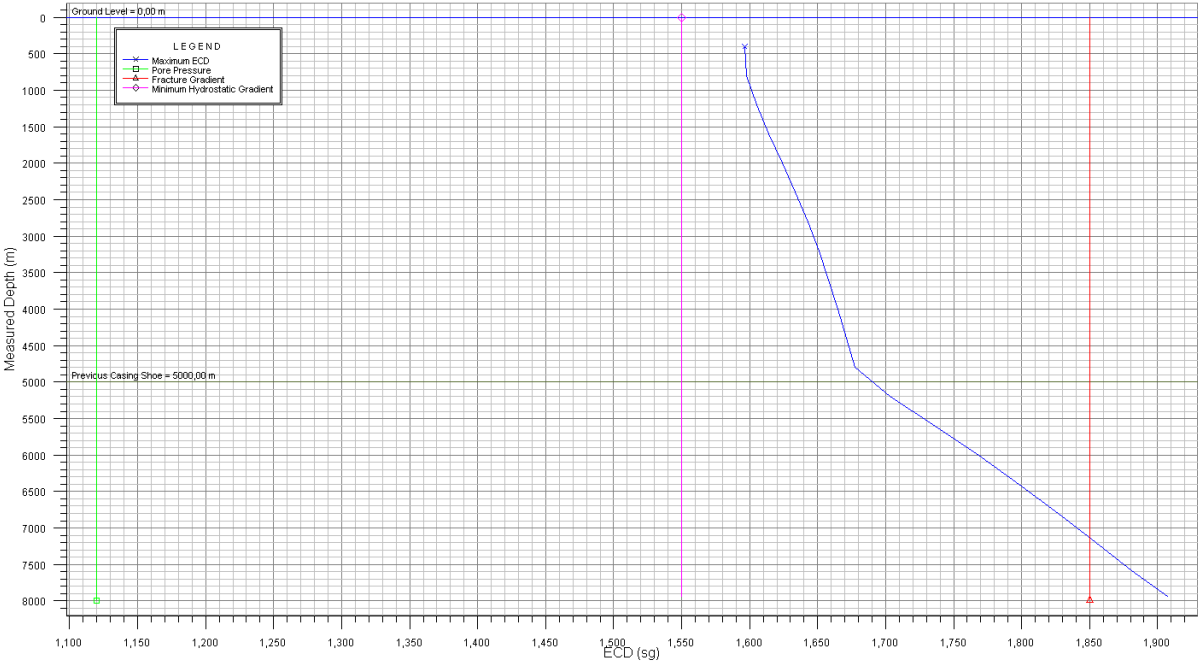


Fig. 4.11 Maximum downhole pressure profile for the cement job for displacement at 1,000 l/min

Simulation #2.4

The viscosity and density of cementing fluids are reduced to see how this will affect the ECD. The viscosity is reduced by a factor of 0.80 from the fluids in **Table 4.7**. The new rheology and density is given in **Table 4.11**.

By comparing **Fig 4.12** with **Fig 4.11**, one can see that a reduction of density and viscosity has a significantly effect on the ECD. However, the formation will still fracture. If it's possible within the operational limits, the density and viscosity can be reduced even more.

Simulation #2.5 will, however, study the affect by shorten the length of the cemented section.

Table 4. 11- Fluid rheology and density

Mud		Spacer		Cement	
Fann Data		Fann data		Fann Data	
Speed [RPM]	Dial [°]	Speed [RPM]	Dial [°]	Speed [RPM]	Dial [°]
600	69.6	300	47.2	300	60.8
300	40.0	200	39.6	200	44.8
200	29.6	100	30.0	100	31.2
100	19.2	60	25.2	60	24.8
6	5.6	30	21.2	30	20.4
3	4.8	6	15.2	6	15.2
		3	14.8	3	13.6
Density [s.g.]		Density [s.g.]		Density [s.g.]	
1.30		1.35		1.40	

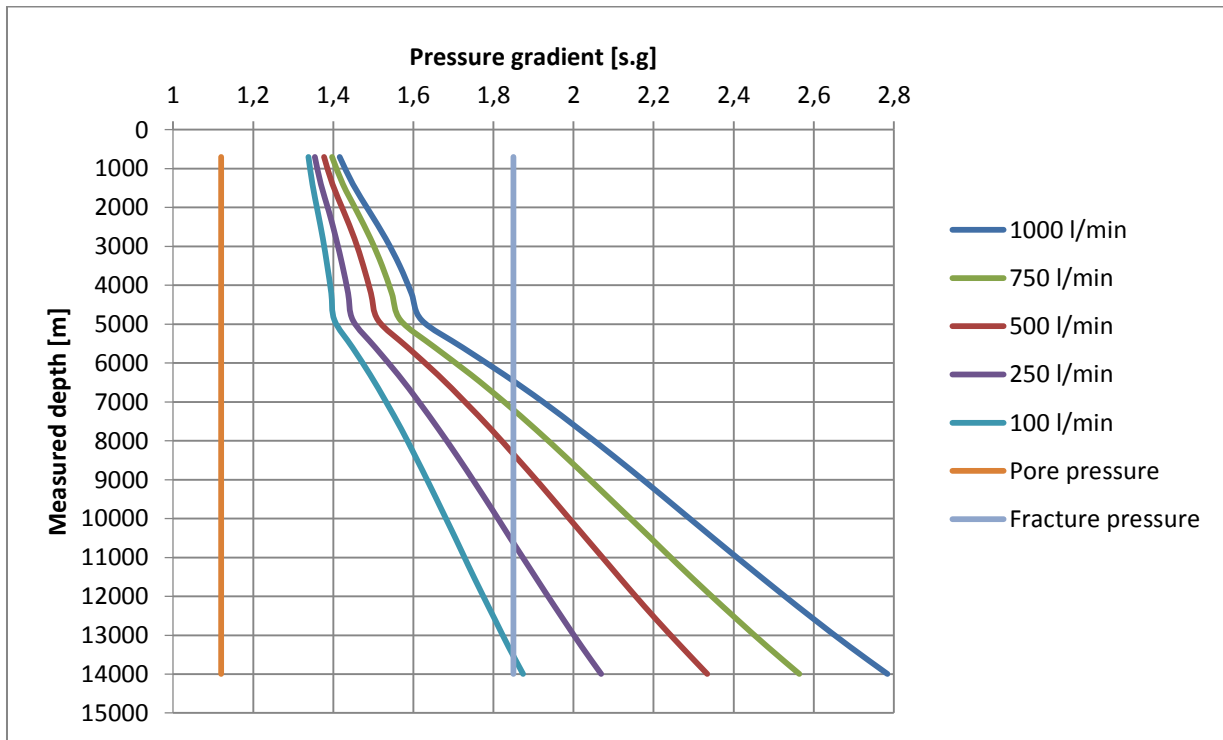


Fig 4.12 Maximum ECD for various flow rates

Simulation #2.5

Originally, the plan is to cement from the bottom of the well to the previous casing shoe (length of 9,000 m). Given that the fluids from **Table 4.11**, the maximum cemented length for various flow rates are given in **Fig 4.13**. Note that the flow rate must be 85 l/min to cement the originally planned cement length of 9,000 m, and a flow rate of 360 l/min only allows a cementation length of 100 m. **Fig 4.14** is a plot of maximum cemented length vs. flow rate. Note that the curve is almost linear.

The **Simulation #2.5** shows that the cementing job can be done changing the fluids (viscosity and density), limit the flow rate, and reducing the length of the cemented section

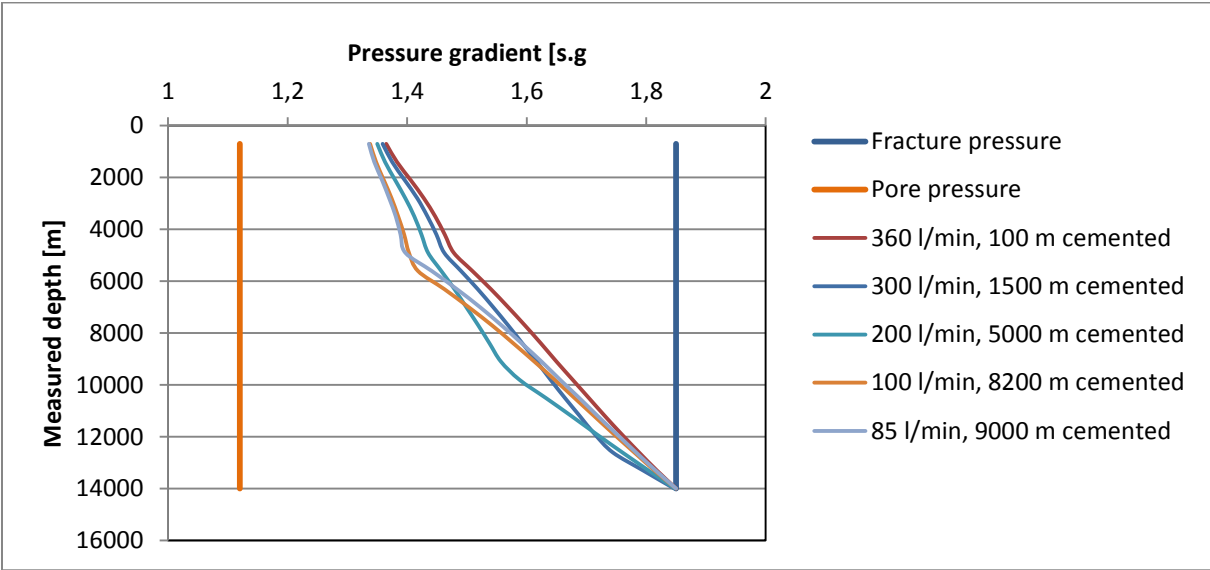


Fig 4.13 Maximum cemented section for different flow rates.

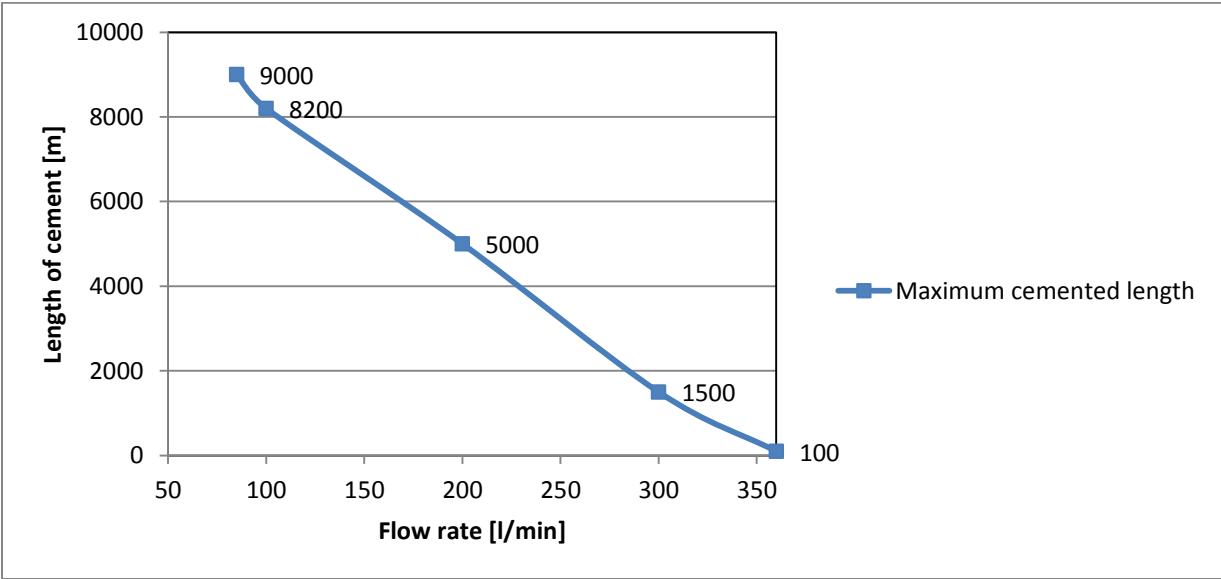


Fig 4.14 Maximum cemented length for different flow rates

4.2 Simulation study installation and cementation of 7” casing

The main objective of this part is to show how the installation of 7” liner is possible; with respect to drill string mechanic to make sure that the drag is within the operational limits (buckling and tensile). The torque is not evaluated in the simulation.

During simulation various operation parameters will be evaluated. These parameters are RPM, running speed, and coefficient of friction.

4.2.1 Simulation of installation 7” casing

4.2.1.1 Simulation arrangement

Table 4.12 show the hole section. The previous set casing is a 10 ¾” casing with the casing shoe at 14,000 m MD. The open hole section where the liner will be installed is from 14,000 – 15,800 m MD.

Table 4.13 show drill string arrangement for the installation of the 7” liner. The 1,800 m liner (named “Casing” under Section Type) is set in the open hole section.

Table 4.14 gives other important data for the simulation.

Fig 4.15 illustrates the well including the drill string arrangement.

Fig 4.16 illustrates the vertical section of the well.

Table 4.12. Hole section

Section Type	MD [m]	Length [m]	ID [in]	Drift [in]	Effective Hole Diameter [in]	Item Description
Casing	14,000	14,000	9.850	9.694	12.715	10 ¾ in, 51 ppf, N-80
Open Hole	15,800	1,800	9.500		9.500	

Table 4.13. Drill string arrangement

Section Type	Length [m]	OD [in]	ID [in]	Item Description
Drillpipe	14,000	6.625	5.901	6 5/8 in, 27.70 ppf, G
Casing	1,800	7.000	6.094	7 in, 32 ppf, N-80

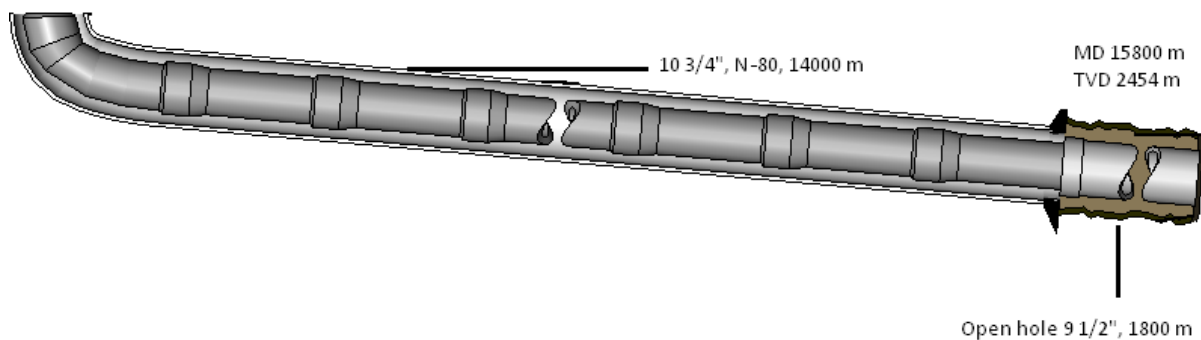


Fig 4.15 Schematic of hole section and drill string arrangement

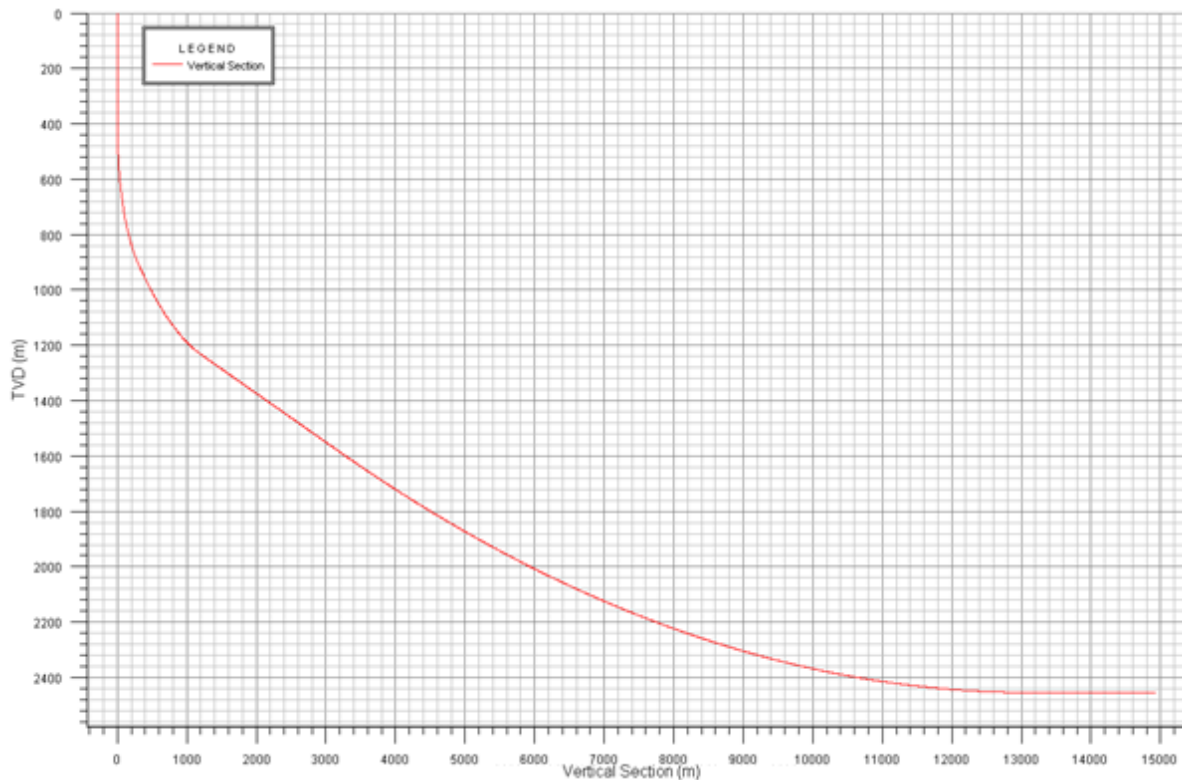


Fig. 4.16 Vertical section of the well

Table 4.14. Parameters for the simulation

Parameter:	Value:
Pump flow rate	500 l/min
Mud density	1.55 s.g.

4.2.1.2 Simulation result

The following three simulations show that, the liner can safely be installed within the buckling and tensile limit by controlling the operational parameters such as RPM and friction coefficient. The maximum running speed for tripping in or tripping out is a function of these two operational parameters (Aadnoy et al., 2010).

Simulation #3.1:

The tripping in/out and the friction factor is given according to **Table 4.15**. At this speed the whole 15,800 m string is tripped in or out by 28.8 hours, which is quite a long time and give high cost to the company.

Fig 4.17 gives the tension for tripping in and tripping out for three different RPM and speed. From the figure one can see that for no 0 RPM, the string will buckle helical for tripping in, and break by tension for tripping out.

Fig 4.17 shows that the limit for Sinusoidal buckling is 20 RPM at tripping in, and the limit for breaking by tension when tripping out is 6 RPM. A third simulation of 60 RPM can also

be seen in the figure. As expected, and discussed in chapter 4.1.1 Simulation of 10 3/4" casing installation, an increase of ROP is improving the safety factor of tripping in/out.

Another simulation is done to see how the installation can be done with a higher trip in or trip out speed. This lead to **Simulation #3.2**

Table 4.15. Simulation parameters

Parameter:	Value:
Friction factor Cased Hole	0.20
Friction factor Open Hole	0.30
Tripping In/Out speed	30 ft/min

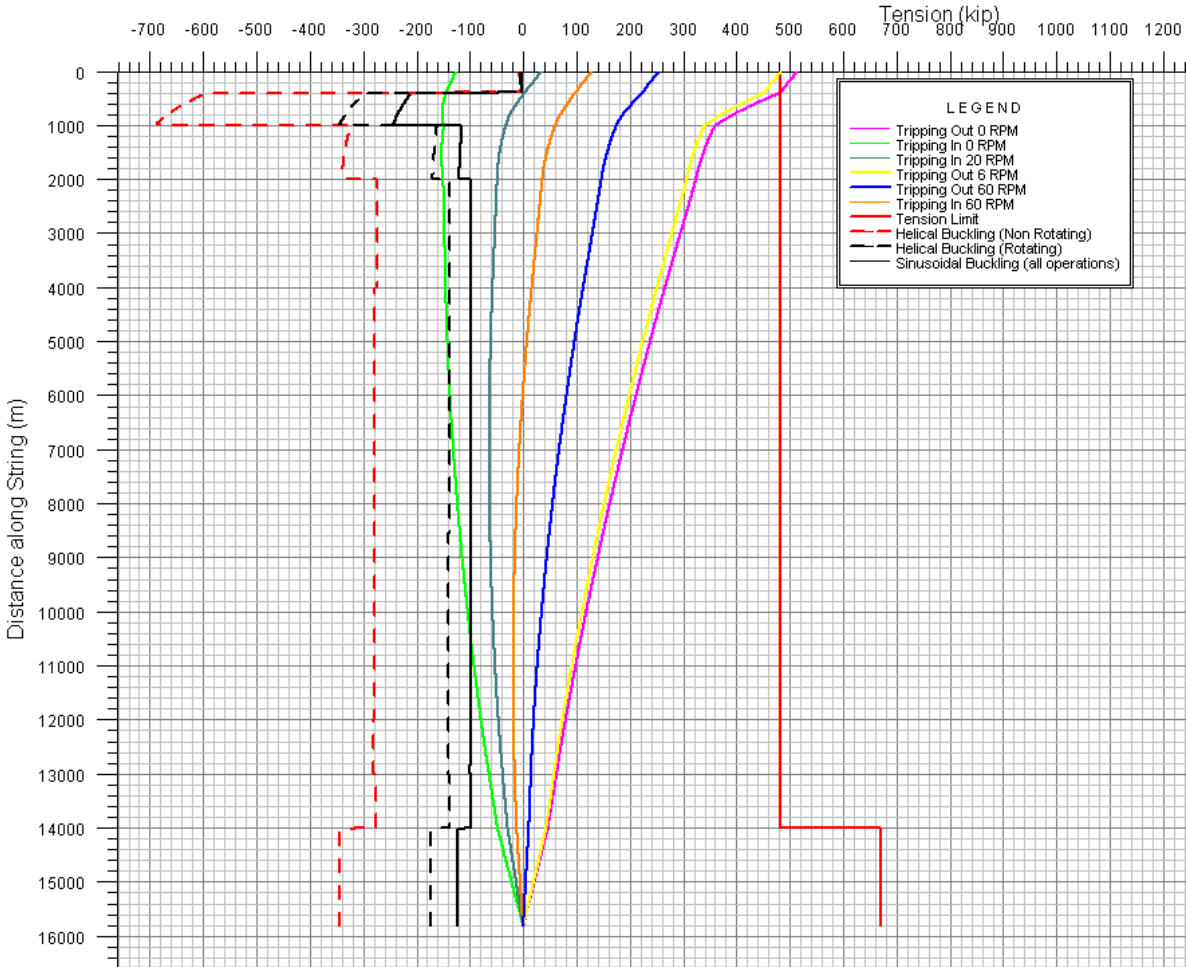


Fig 4.17 Effective tension by tripping in/out for various RPM

Simulation #3.2

The trip in, trip out and friction factor is set according to **Table 4.16**. At this speed the whole 15800 m string is tripped in or out by 14.4 hours.

Fig 4.18 gives the tension for tripping in and tripping out for three different RPM. As expected the 0 RPM curve in this simulation is the same as in **Simulation #3.1 (Fig 4.17)**

Fig 4.18 show that the limit to avoid Sinusoidal Buckling by tripping in is 40 RPM, and the limit to avoid tensional breaking by tripping out is 13 RPM. By theory, the tripping out limit should be twice the limit as simulated in **Simulation #3.1**. One must assume that this is due to number of significant digits and rounding of the digits.

By comparing the tripping in/out 60 RPM of **Fig 4.18** and **Fig 4.17** one can see that the increase of running is reducing the safety factor for buckling or breaking by tension.

It's seen that an increase of RPM is decreasing the friction between the drill string and the wellbore. The friction can also be reduced by reducing the friction factor of the casing and the open hole. This leads to **simulation #3.3**.

Table 4.16.Simulation parameters

Parameter:	Value:
Friction factor Cased Hole	0.20
Friction factor Open Hole	0.30
Tripping In/Out speed	60 ft/min

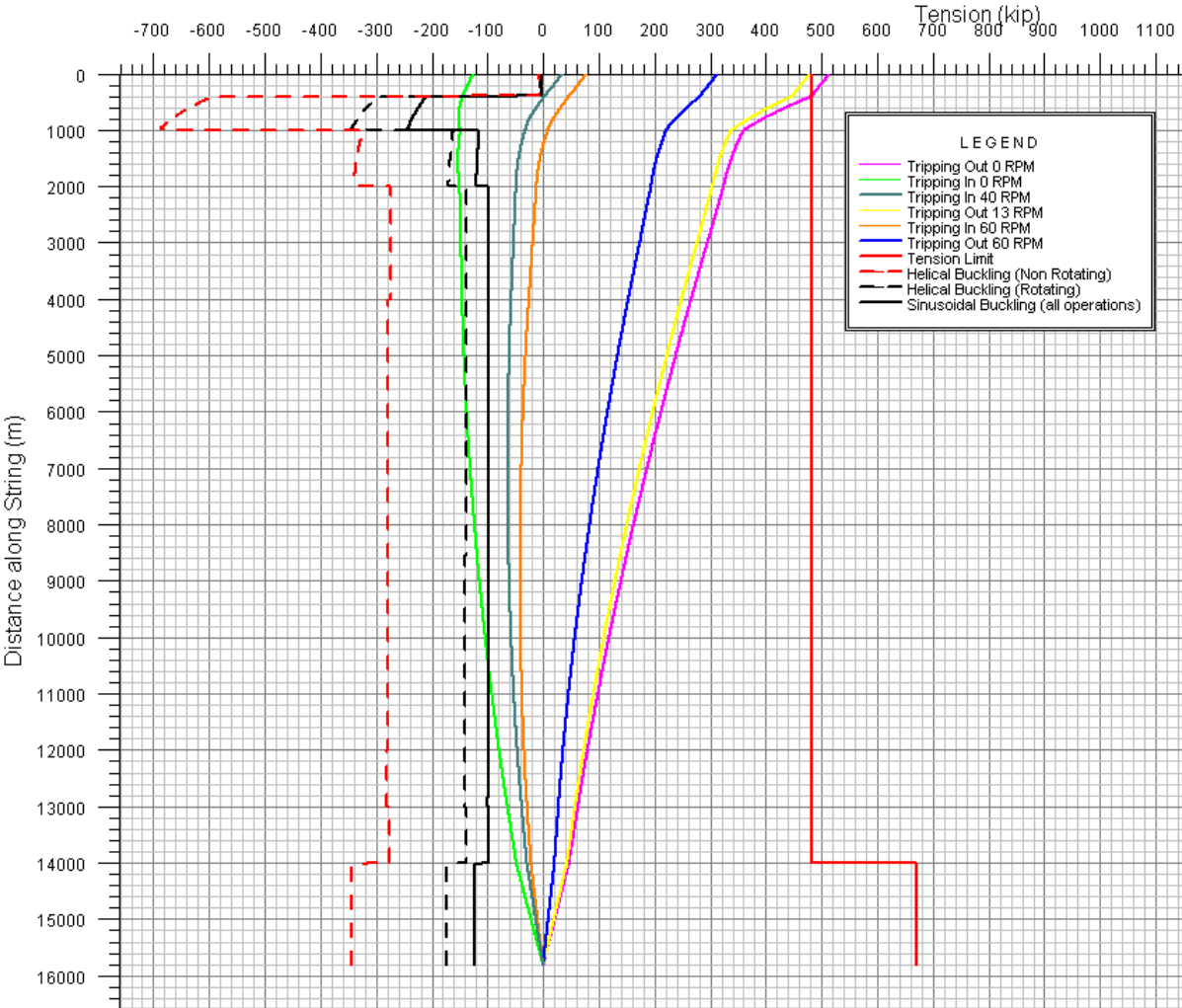


Fig 4.18 Effective tension for various RPM

Simulation #3.3

In this simulation, the running speed and RPM is constant, while the friction factor is changed between the three different cases. These simulation parameters are given in **Table 4.17**.

Fig. 4.19 show, as expected, that a change of the friction factor will change the tension by tripping in and tripping out. By comparing **Fig 4.19** with the **Fig 4.6**, one can see that a change in friction factor for the liner installation has a larger affect, than for the casing installation.

Table 4.17. Simulation parameters

	Parameter:	Value:
	Tripping In/Out speed	60 ft/min
	RPM Tripping In/Out	60 RPM
Case 1	Friction factor Cased Hole	0.20
	Friction factor Open Hole	0.30
Case 2	Friction factor Cased Hole	0.15
	Friction factor Open Hole	0.25
Case 3	Friction factor Cased Hole	0.10
	Friction factor Open Hole	0.20

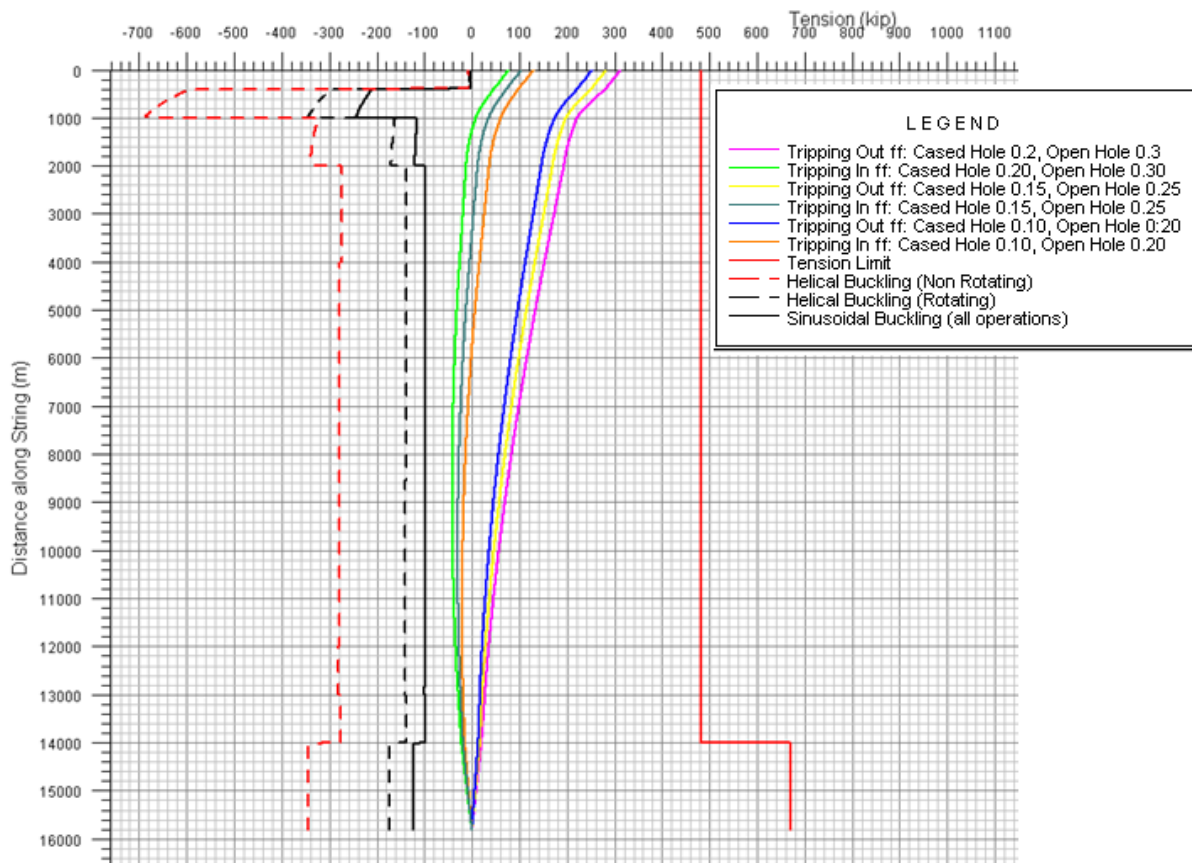


Fig 4.19 Effective tension by tripping in/out for various friction coefficients

4.2.2 Simulation of cementation 7" casing

4.2.2.1 Simulation arrangement

The fluids in this simulation are the same as for the 10 3/4" cementing and can be found in **Table 4.7** and **4.11**.

Fig 4.20 shows the pore and fracture pressure vs. MD for the well. Note that the figure gives what the actual pressure is in bar, and not the gradient. The figure also gives the information of the pore pressure gradient and fracture pressure gradient.

Fig 4.21 shows an illustration of how the cement is displaced and set in the annulus between the liner and the wellbore wall. The cement is pumped inside the drillpipe to the bottom of the well, and will then go up the annulus between the liner and wellbore wall. The total length of the liner will be cemented (1,800 m).

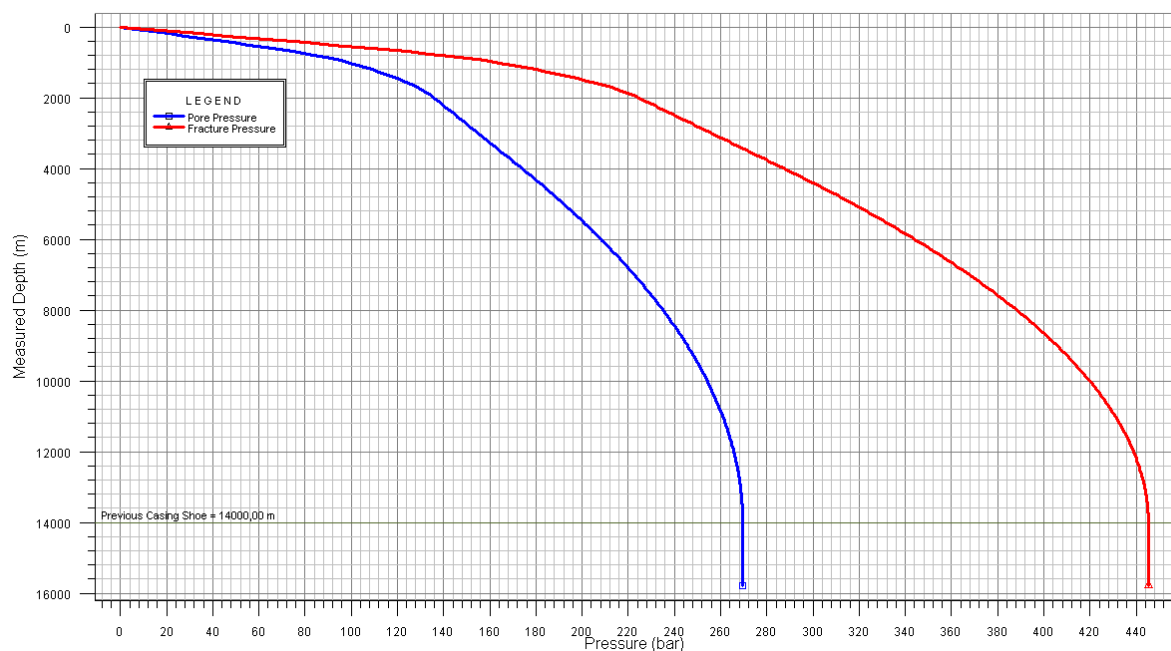


Fig 4.20. Pore and Fracture pressure

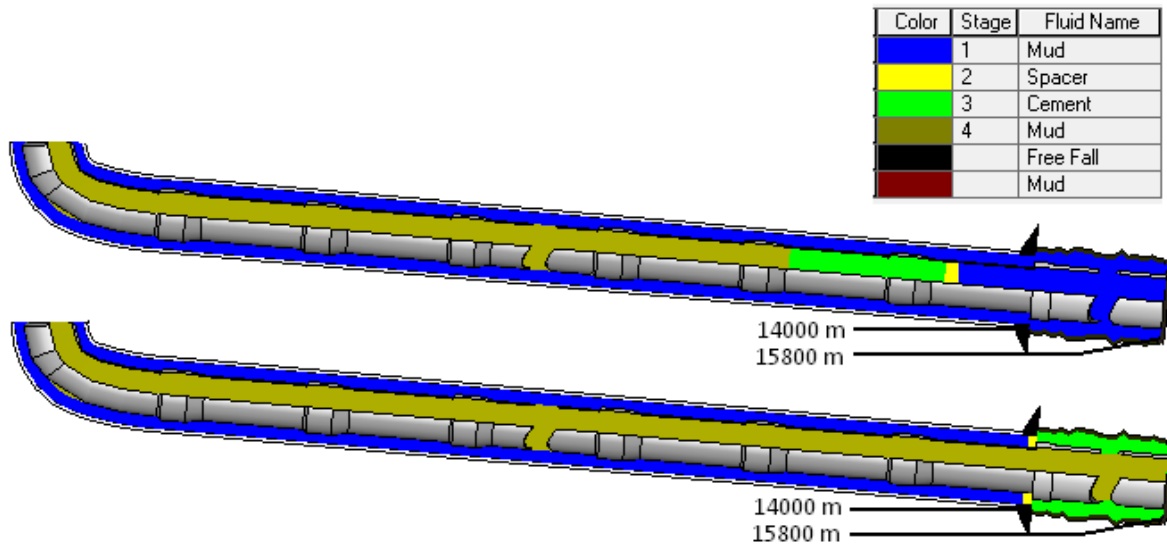


Fig 4.21 Schematic figure of the cementing job

4.2.2.2 Simulation result

The following two simulations show that the cementing job can be done by changing the operation parameters. The density and rheology of the cementing fluids, and the flow rate has a great influence on the frictional pressure loss. By reducing the density and viscosity of the cementing, the flow rate during circulation can be quite high without fracturing the formation,

Simulation #4.1

This simulation is done with the fluids from **Table 4.7** at different flow rates. **Fig 4.22** show that the upper limit of flow rate for this cementing job is 500 l/min. The displacement time for various flow rates are found in **Table 4.18**.

It's preferred to keep the flow rate as high as possible. Simulation #4.2 is done to see if a higher flow rate can be achieved by a reduction of the density and viscosity of the cementing fluids.

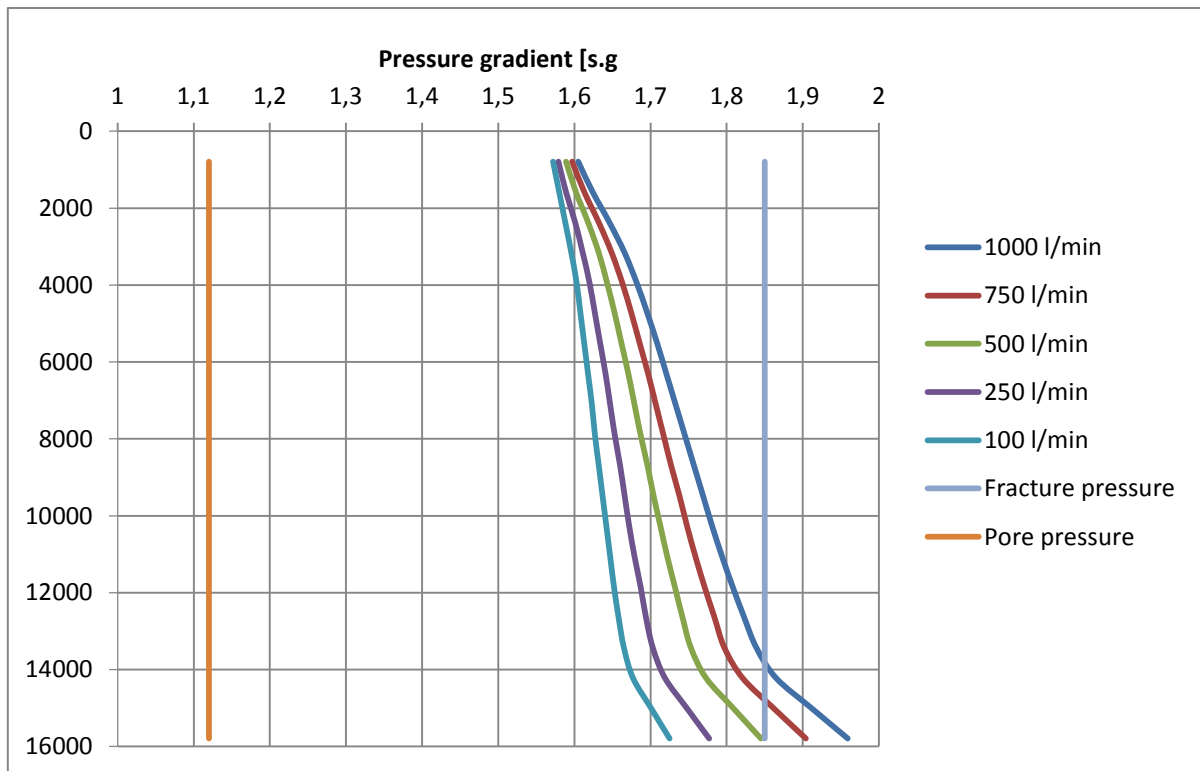


Fig 4.22 Maximum ECD for different flow rates

Table 4. 18. Time duration for different flow rates

Flow rate [l/min]:	Duration [hours]:
1000	5.4
750	8.0
500	10.7
250	21.4
100	53.6

Simulation #4.2

This simulation is done with the fluids from **Table 4.11**. With a reduction of the density and viscosity of the cementing fluids, one can see from **Fig. 4.23** that the upper limit to avoid formation fracture is 2,400 l/min. At this flow rate, the time duration for cement displacement is only 2.2 hours.

The flow rate of 2,400 l/min is quite high. Possible, one should question this result. However, the length of the cemented section is only 1,800, compared to 9,000 m for cementing of casing. One should also remember that the hydraulic diameter is larger for the liner installation, comparing to the casing installation. These factors give a reduction of frictional pressure loss for the liner installation compared to the casing installation. By comparing the hydraulic diameter of the liner and the casing, simple calculations show that the hydraulic diameter is 20% larger at the liner section, and 34% larger above the liner. It seems like the geometry has a significant impact on the pressure loss.

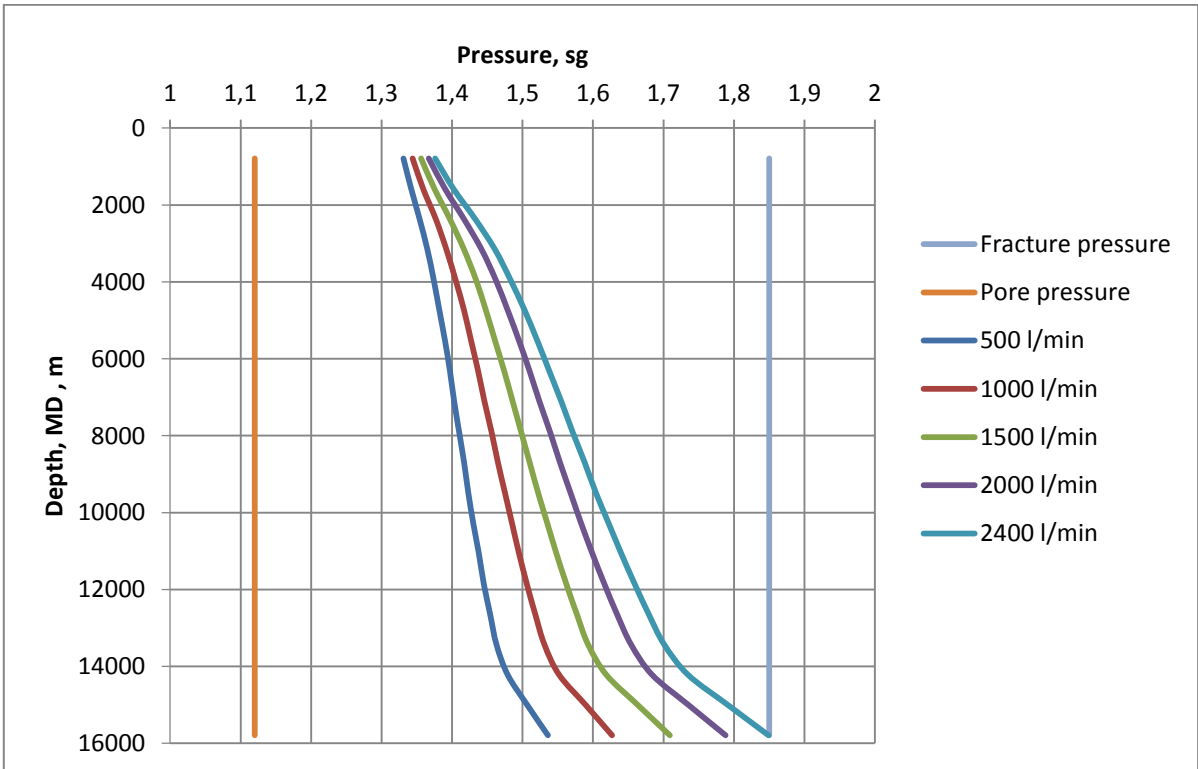


Fig 4.23 Maximum ECD for different flow rates

5 Simulation study of cementation of 10 3/4" casing using MATLAB

The WELLPLAN simulator is only giving an output like **Fig 4.11** and it's difficult to say if the simulation by WELLPLAN is correct, as the source code and calculations behind the simulations are not given to the user.

A simulation study with MATLAB is therefor used to compare the results from chapter 4.12.2 Simulation of cementation of 10 3/4" casing. With the written MATLAB code, the equations and calculations are open and available to the user.

The ECD is also affected by which rheology model which is used. This study will also compare the difference between three different rheology models (Bingham, Power Law, and Herschel-Bulkley).

5.1 Simulation arrangement

The MATLAB code for the simulation are given in Appendix C.

The following assumption is made to reduce the complexity of the MATLAB code.

- Fluid properties (rheology and density) are the same for all fluids in the well. I.e. the cement, spacer and mud have the same viscosity and density.
- The wellbore geometry is the same through the whole length of the well.

Three simulations are studied in this chapter. The well geometry, MD and TVD are given in **Table 4.19**. Note that the MD and TVD is the same as for WELLPLAN simulations.

The only parameter that is changed between the three different simulations is the fluid density and rheology.

Table 4. 19 Well data for simulation

Parameter:	Value:
Wellbore diameter	12 1/4"
Casing outer diameter	10 3/4"
Casing inner diameter	9.85"
Measured depth	14,000 m
True vertical depth	2,454 m

5.2 Simulation results

Based on the simplicity assumption of the MATLAB analysis, one cannot conclude that the cementing operation can safely be executed with the result in the following three MATLAB simulations. This is due to the simplicity assumptions of constant well geometry and constant fluid properties for all three cementing fluids. However, this study is done to show that the different fluid rheology models can give significantly different results

Simulation #5.1

This simulation is a worst case scenario, where the mud, spacer, and cement have its rheology and density as the cement given in **Table 4.20**.

Fig 4.24 shows that the ECD is greatly affected by which rheology model that is used. Therefore it's crucial to decide the best fitted rheology model of the fluids in the cementing operation, in order to get correct simulations. The only operation parameter that gives a safe operation is the 100 l/min Power law.

The maximum ECD for 100 l/min in this simulation and **Simulation #2.2** from chapter 4.1.2.2 Simulation is given in **Table 4.21**. It can be seen from the table that the WELLPLAN give a maximum ECD which is just below the Bingham and Herschel-Bulkley.

Unlike the curves from WELLPLAN simulations (e.g. **Fig 4.11**), the curves are linear. The reason of this is that WELLPLAN can simulate for different wellbore geometry, where the geometry is changed at the casing shoe. The MATLAB code is using the same wellbore geometry for the entire well

Table 4. 20. Fluid data

Speed [RPM]	Dial [°]	Densiry [s.g.]
600	134	1.60
300	76	
200	56	
100	39	
6	19	
3	17	

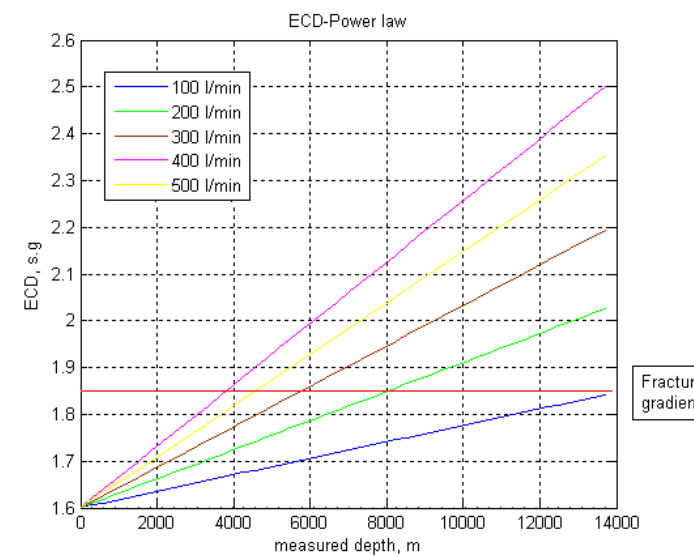
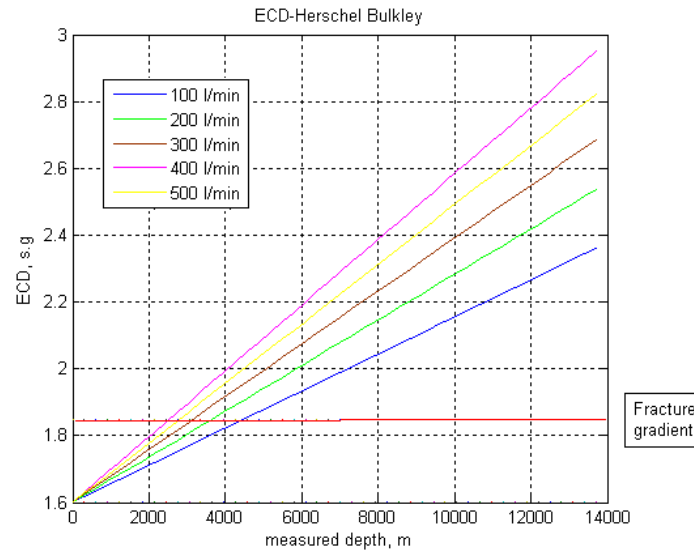
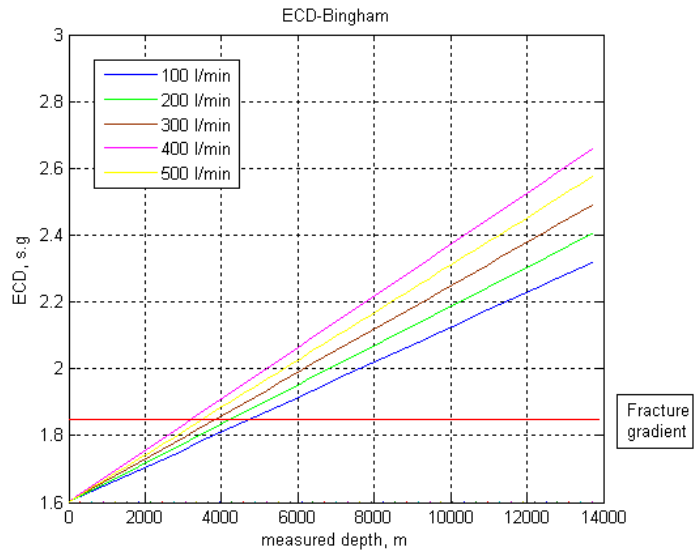


Fig 4. 24 ECD for three different rheology models

Table 4. 21. Maximum ECD for different rheology models

Rheology model	Software	Maximum ECD [s.g.]
Bingham	MATLAB	2.32
Herschel-Bulkley	MATLAB	2.38
Power law	MATLAB	1.84
Generalized Herschel-Bulkley	WELLPLAN	2.25

Simulation #5.2

In this simulation, the viscosity and density are reduced according to **Table 4.22**. The data in this table is the weighted average from the fluids in **Table 4.7** to give a more realistic data of the fluid.

The maximum ECD for various flow rates can be seen in **Fig 4.25**. For 500 l/min in this simulation and **Simulation #2.2** from chapter 4.1.2.2 Simulation is given in **Table 4.23**. It can be seen from the table that the WELLPLAN give a maximum ECD which is quite higher than the other three models.

The only operation parameter that gives a safe operation is the 100 l/min Power law. The fluid rheology and density must be reduced even more. This leads to **Simulation #5.3**.

Table 4.22 Fluid rheology and density

Speed [RPM:]	Dial [°]	Density [s.g.]
600	97.8	1.56
300	56.0	
200	41.4	
100	27.5	
6	9.8	
3	8.6	

Table 4. 23 Maximum ECD for different models

Rheology model:	Software:	Maximum ECD [s.g.]
Bingham	MATLAB	2.37
Herschel-Bulkley	MATLAB	2.44
Power law	MATLAB	2.24
Generalized Herschel-Bulkley	WELLPLAN	2.81

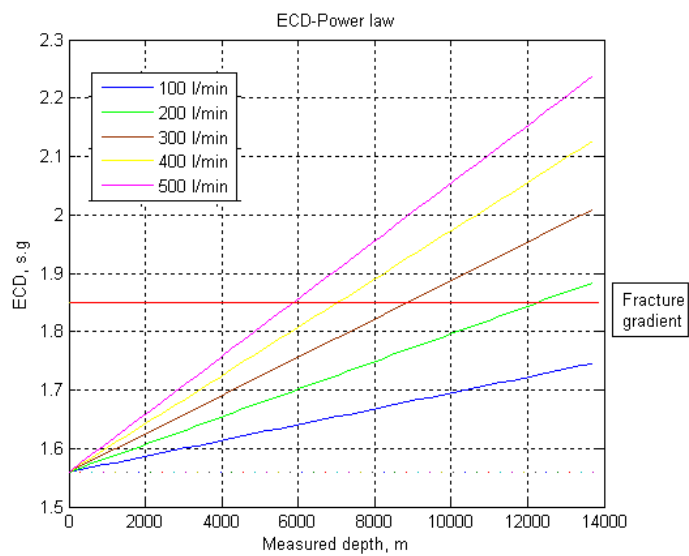
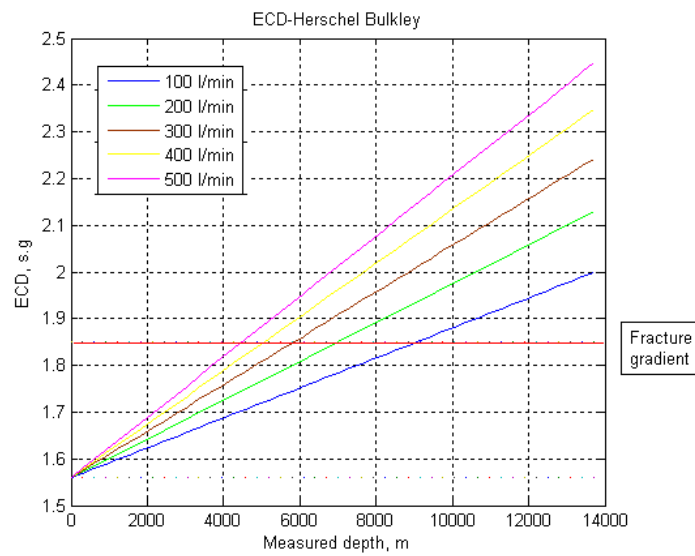
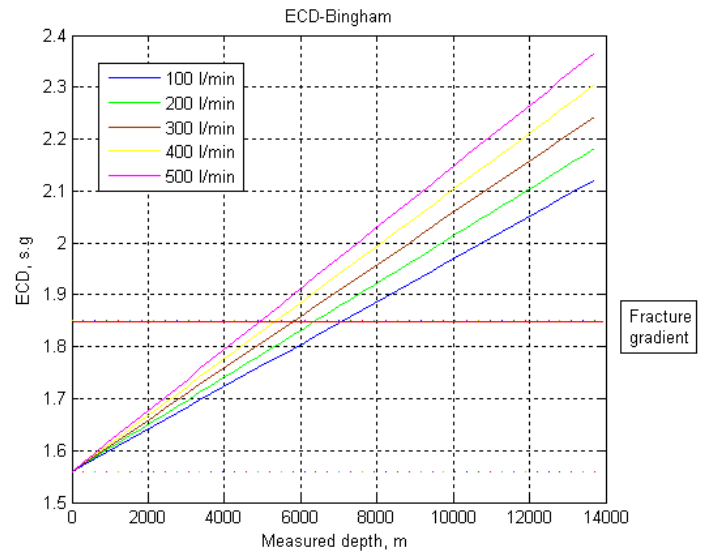


Fig 4.25 ECD for three different rheology models

Simulation #5.3

The fluid data is given in **Table 4.24**. The data is based on the weighted average of the fluids in **Table 4.11**.

Fig 4.26 shows that a flow rate of 200 l/min is safe for all three models. The results from **Simulation #2.5** in chapter 4.1.2.2 show that both 200 l/min and 100 l/min would fracture the formation.

Table 4.24. Fluid rheology and density

Speed [RPM]:	Dial [°]:	Density [s.g.]
600	72.8	1.32
300	44.8	
200	33.1	
100	22.0	
6	7.8	
3	6.9	

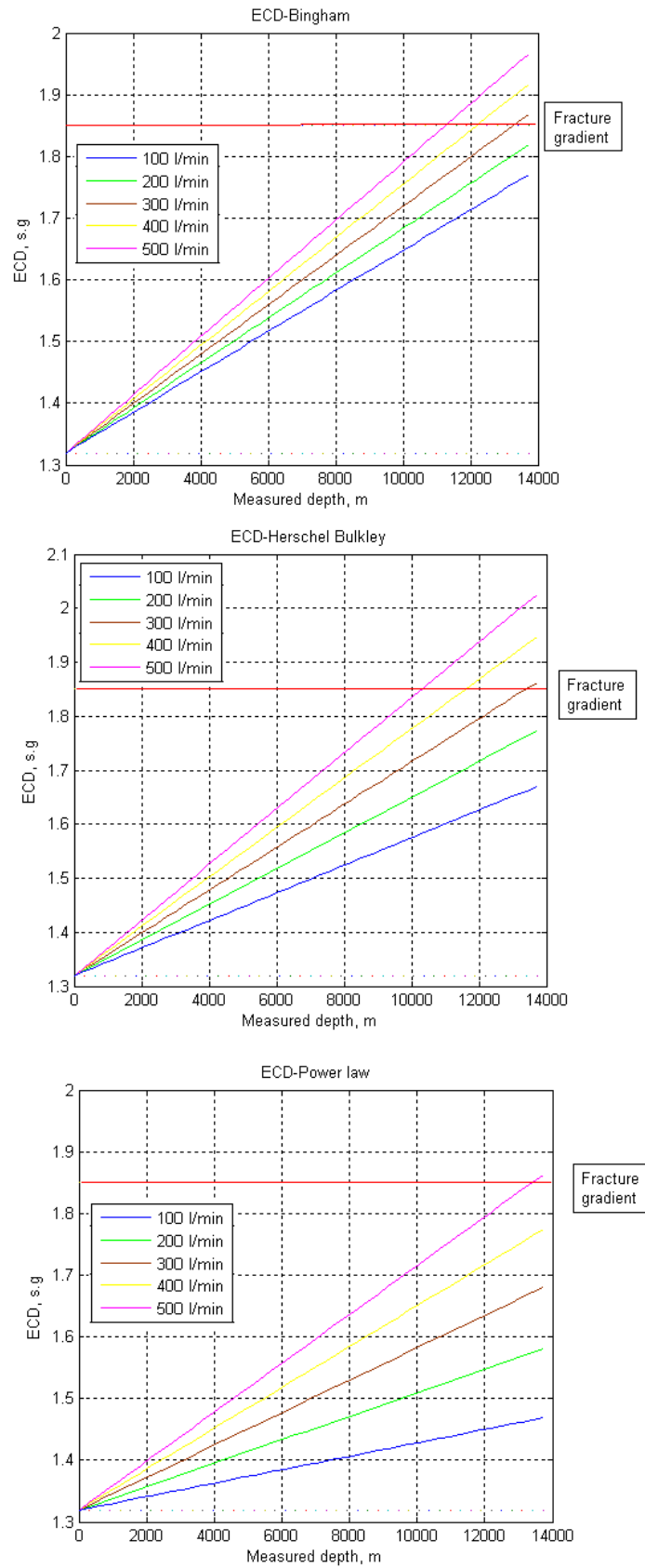


Fig 4. 26 ECD for three different rheology models

6 Summary and discussion

The simulation and case studies in this thesis show that the 10 3/4" casing and 7" liner can be installed and cemented by controlling the operational parameters.

Installation of 10 3/4" casing

- The WELLPLAN simulation result shows that the drag forces under tripping in or tripping out can be kept within the buckling and tensile limit. This is done by controlling friction coefficient and the operation parameters such as RPM and running speed.
- Given a friction coefficient of 0.20 for cased hole, and 0.30 for open hole. The casing string can be tripped out without any rotation of the string, within the tensional limits.

Cementation of 10 3/4" casing

The simulation by WELLPLAN shows that: the ECD is affected by:

- the flow rate,
- the length of the well,
- geometry of the wellbore,
- the rheology and density of the cementing fluids, and
- the length of the cemented section

Possible the most important parameter to evaluate is the rheology and density of the cementing fluids.

The simulation with MATLAB shows that the ECD calculations are depending on which rheology model that is used. It's very important perform laboratory tests to decide which model that is the best fit for the fluids. It's difficult to compare the results between the MATLAB and the WELLPLAN as different rheology models was used, and the MATLAB could not handle 3 different kind of fluids

Installation of 7" liner

- The WELLPLAN simulation result shows that the drag forces under tripping in or tripping out can be kept within the buckling and tensile limit. This is done by controlling
-

Cementation of 7" liner

- The simulation with WELLPLAN show that the cementing operation can be done without too much tweaking of the parameters (fluid rheology, flow rates, etc).

7 Further work

The following are suggested for further work:

Installation of casing and liner

- Torque analysis.
- Analyze the possibility of drilling with liner.

Cementation

- Simulation with different well geometry.
- Simulations with different fluid rheologies.
- Simulation with other cementing techniques like pumping down cement down the annulus, multistage cementing, and Managed Pressure Drilling (MPD) cementing
- Laboratory tests with different fluid.

References

- Aadnoy, B. S., Fazaelizadeh, M., & Hareland, G. (2010). A 3D Analytical Model for Wellbore Friction. *Journal of Canadian Petroleum Technology*, 49(10), pp. 25-36. doi: 10.2118/141515-pa
- Agbaji, A. L. (2010). *Optimizing the Planning, Design and Drilling of Extended Reach and Complex Wells*. Paper presented at the Abu Dhabi International Petroleum Exhibition and Conference, Abu Dhabi, UAE.
<http://www.onepetro.org/mslib/app/Preview.do?paperNumber=SPE-136901-MS&societyCode=SPE>
- API. (2010). Recommended Practice 13 D: Rheology and Hydraulics of Oil-well Drilling Fluids. 6th.
- Azar, J. J., & Samuel, G. R. (2007). *Drilling engineering*. Tulsa, Okla.: PennWell Corp.
- Belarde, M. A., & Vestavik, O. M. (2011). *Deployment of Reelwell Drilling Method in Shale Gas Field in Canada*. Paper presented at the Offshore Europe, Aberdeen, UK.
<http://www.onepetro.org/mslib/app/Preview.do?paperNumber=SPE-145599-MS&societyCode=SPE>
- Bourgoyne, A. T. (1991). *Applied drilling engineering* (Vol. Vol. 2). Richardson, TX: Society of Petroleum Engineers.
- Byrom, T. G. (2007). *Casing and liners for drilling and completion*. Houston, Tex: Gulf Pub.
- Chen, H. J., Fu, B., Rey, D., Kouba, G. E., & Fouchi, M. S. (2000). *Field Application of a Drag Reducing Agent to Increase Gas Production*.
<http://www.onepetro.org/mslib/app/Preview.do?paperNumber=NACE-00073&societyCode=NACE>
- Devereux, S. (2012). *Drilling technology in nontechnical language*. Tulsa, Okla.: PennWell.
- Gucuyener, I. H. (1983). *A Rheological Model for Drilling Fluids and Cement Slurries*. Paper presented at the Middle East Oil Technical Conference and Exhibition, Bahrain.
<http://www.onepetro.org/mslib/app/Preview.do?paperNumber=00011487&societyCode=SPE>
- Hibbeler, J., Rae, P., Gilmore, T., & Weber, L. (2000). *Using Alternative Sources of Oilwell Cement*. Paper presented at the IADC/SPE Asia Pacific Drilling Technology, Kuala Lumpur, Malaysia.
<http://www.onepetro.org/mslib/app/Preview.do?paperNumber=00062746&societyCode=SPE>
- Hjelle, A., Teige, T. G., Rolfsen, K., Hanken, K. J., Hernes, S., & Huelvan, Y. (2006). *World-Record ERD Well Drilled From a Floating Installation in the North Sea*. Paper presented at the IADC/SPE Drilling Conference, Miami, Florida, USA.
<http://www.onepetro.org/mslib/app/Preview.do?paperNumber=SPE-98945-MS&societyCode=SPE>
- Johancsik, C. A., Friesen, D. B., & Dawson, R. (1984). Torque and Drag in Directional Wells—Prediction and Measurement. *Journal of Petroleum Technology*, 36(6), 987-992. doi: 10.2118/11380-pa
- Mason, C. J., & Judzis, A. (1998). *Extended-Reach Drilling -- What is the Limit?* Paper presented at the SPE Annual Technical Conference and Exhibition, New Orleans, Louisiana.
<http://www.onepetro.org/mslib/app/Preview.do?paperNumber=00048943&societyCode=SPE>
- Merlo, A., Maglione, R., & Piatti, C. (1995). *An Innovative Model For Drilling Fluid Hydraulics*. Paper presented at the SPE Asia Pacific Oil and Gas Conference, Kuala Lumpur, Malaysia.

<http://www.onepetro.org/mslib/app/Preview.do?paperNumber=00029259&societyCode=SPE>

Mitchell, R. F., & Miska, S. (2011). *Fundamentals of drilling engineering*. Richardson, Tex.: Society of Petroleum Engineers.

Nelson, E. B., & Guillot, D. (2006). *Well Cementing*. Sugar Land, Tex.: Schlumberger.

Time, R. W. (2009). *Two-phase Flow in Pipelines, course compendium*

Vestavik, O. M., Brown, S. C., & Kerr, S. P. (2009). *Reelwell Drilling Method*. Paper presented at the SPE/IADC Drilling Conference and Exhibition, Amsterdam, The Netherlands. <http://www.onepetro.org/mslib/app/Preview.do?paperNumber=SPE-119491-MS&societyCode=SPE>

Viloria, O. M. (2006). Analysis of drilling fluid rheology and tool joint effect to reduce errors in hydraulics calculations.

White, G. L. (1964). *Friction Pressure Reducers in Well Stimulation*.

Zamora, M., Sanjit, R., & Slater, K. (2005). *Comparing a Basic Set of Drilling Fluid Pressure-Loss Relationships to Flow-Loop and Field Data*. Paper presented at the AADE 2005 National Technical Conference and Exhibition, Houston.

Appendix A: Hydraulics models

In this section, the Bingham (Bourgoyne, 1991), Power law (Bourgoyne, 1991), Herschel-Bulkley (Merlo, Maglione, & Piatti, 1995) (Zamora, Sanjit, & Slater, 2005), and Newtonian models (Time, 2009) are presented. These equations are used in the MATLAB code to calculate frictional pressure loss and ECD

A.2 Bingham Plastic fluid

Pipe flow

$$\mu_a = \mu_p + \frac{5\tau_y d}{v_p}$$

Annulus

$$\mu_a = \mu_p + \frac{5\tau_y(d_2-d_1)}{v_a}$$

A.3 Power law fluid

Pipe flow:

The Reynolds number:

$$N_{re} = \frac{89100\rho v_p^{(2-n)}}{k} \left(\frac{0,0416d}{3+n^{-1}} \right)^n$$

where,

$$n = 3.32 * \log \frac{\theta_{600}}{\theta_{300}}, \text{ and}$$

$$k = 510 * \frac{\theta_{300}}{511^n}$$

For laminar flow, $N_{ReC} = 3470-1370n$.

For turbulent flow, $N_{ReC} = 4270-1370n$.

If $N_{Re} < N_{ReC} \rightarrow$ laminar flow

$$\Delta P = \frac{K v_p^n \Delta L \left(\frac{3+n^{-1}}{0,0416} \right)^n}{144000 d_p^{(1+n)}}$$

If $N_{Re} > N_{ReC} \rightarrow$ turbulent flow

$$\Delta P_f = \frac{f v_p^2 \rho}{25,81(d_2-d_1)} \Delta L$$

$$f = a N_{re}^{-b}$$

$$a = \frac{\log n + 3.93}{50}$$

$$b = \frac{1.75 - \log n}{7}$$

Annulus:

$$N_{re} = \frac{109000 \rho v_a^{(2-n)}}{k} \left(\frac{0,0208(d_2-d_1)}{2+n^{-1}} \right)^n$$

For laminar flow, $N_{ReC} = 3470-1370n$.

For turbulent flow, $N_{ReC} = 4270-1370n$.

If $N_{Re} < N_{ReC} \rightarrow$ laminar flow

$$\Delta P = \frac{k v_a^n \left(\frac{2+n^{-1}}{0,0208} \right)^n}{144000 (d_2-d_1)^{1+n}} \Delta L$$

If $N_{Re} > N_{ReC} \rightarrow$ turbulent flow

$$\Delta P_f = \frac{f v_p^2 \rho}{25,81(d_2-d_1)} \Delta L$$

A.4 Herschel-Bulkley fluid

To calculate velocity, follow the procedure in section 2.6.1 (pipe and annulus).

The Reynolds number:

$$N_{re} = \frac{2(3n+1)}{n} \left[\frac{\rho v_p^{(2-n)} \left(\frac{d}{2} \right)^n}{\tau_0 \left(\frac{d}{2 v_p} \right)^2 + K \left(\frac{3n+1}{n C_c} \right)^n} \right]$$

The critical Reynold number to establish if it's laminar or turbulent flow:

$$N_{ReC} = \left[\frac{4(3n+1)}{n y} \right]^{\frac{1}{1-z}}$$

Where $y = \frac{\log n + 3,93}{50}$, and

$$z = \frac{1,75 - \log n}{7}$$

If $N_{Re} < N_{ReC} \rightarrow$ laminar flow

$$\Delta P = \frac{4 k}{14400 d} \left\{ \frac{\tau_0}{k} + \left[\left(\frac{3 n+1}{n C_c} \right) \left(\frac{8 q}{\pi d^3} \right) \right]^n \right\} \Delta L$$

If $N_{Re} > N_{ReC} \rightarrow$ turbulent flow

$$\Delta P = \frac{f q^2 \rho}{1421,22 d^5} \Delta L$$

where $f = y (C_c N_{Re})^{-z}$, and

$$C_c = 1 - \left(\frac{1}{2n+1} \right) \frac{\tau_0}{\tau_0 + k \left[\frac{(3n+1)q}{n \pi \left(\frac{d}{2} \right)^3} \right]^n}$$

Annulus:

The Reynolds number:

$$N_{Re} = \frac{4(2n+1)}{n} \left[\frac{\rho v_a^{(2-n)} \left(\frac{d_2-d_1}{2} \right)^n}{\tau_0 \left(\frac{d_2-d_1}{2 v_a} \right)^2 + K \left(\frac{3n+1}{n C_c} \right)^n} \right]$$

The critical Reynolds number to establish if it's laminar or turbulent flow:

$$N_{Rec} = \left[\frac{8(2n+1)}{n y} \right]^{\frac{1}{1-z}}$$

Where $y = \frac{\log n + 3,93}{50}$, and
 $z = \frac{1,75 - \log n}{7}$

If $N_{Re} < N_{Rec} \rightarrow$ laminar flow

$$\Delta P = \frac{4k}{14400(d_2-d_1)} \left\{ \frac{\tau_0}{k} + \left[\left(\frac{16(2n+1)}{n C_a (d_2-d_1)} \right) \left(\frac{q}{\pi (d_2^2-d_1^2)} \right) \right]^n \right\} \Delta L$$

If $N_{Re} > N_{Rec} \rightarrow$ turbulent flow

$$\Delta P = \frac{f q^2 \rho}{1421,22 (d_2-d_1) (d_2^2-d_1^2)^2} \Delta L$$

Where $f = y (C_a N_{Re})^{-z}$,

$$C_a = 1 - \left(\frac{1}{n+1} \right) \frac{\tau_0}{\tau_0 + k \left[\frac{2(2n+1)q}{n \pi \left(\frac{d_2}{2} \right) \left(\frac{d_1}{2} \right) \left(\left(\frac{d_2}{2} \right)^2 - \left(\frac{d_1}{2} \right)^2 \right)} \right]^n}, \text{ and}$$

$$z = \frac{1,75 - \log n}{7}$$

A.4 Newtonian fluid

The Darcy friction factor is four times greater than the Fanning friction factor. Thus, it's important to be specific of which friction factor one has used for the calculations

Reynolds number

The Reynolds number

$$Re = \frac{\rho u d_H}{\mu}$$

Where ρ is fluid density, u is fluid velocity, d_H is hydraulic diameter, μ is fluid viscosity, q is volumetric flow rate and A is cross-sectional area

. The flow regime is determined by the Reynolds number as following:

- $Re \leq 2000$: laminar flow.
- $2000 < Re \leq 4000$: transition between laminar and turbulent flow.
- $4000 < Re$: turbulent flow.

Friction factor laminar flow

For a single phase laminar flow the Fanning friction factor is mathematically given by:

$$f_f = \frac{16}{Re} \quad (\text{Fanning})$$

Several different equations for Darcy friction factor exists. Haaland (1983) is one equation which is often used:

$$\frac{1}{\sqrt{f_d}} \approx -1.8 \log \left(\left(\frac{\epsilon/D}{3.7} \right)^{1.11} + \frac{6.9}{Re} \right) \quad (\text{Darcy})$$

Where f_d is Darcy friction factor, ϵ/D is relative roughness of the pipe and Re is Reynolds number.

Friction factor turbulent flow

$$f_f = 0.079 Re^{-0.25} \quad (\text{Blasius}) \quad (\text{Fanning})$$

$$f_f = 0.046 Re^{-0.2} \quad (\text{Dukler}) \quad (\text{Fanning})$$

$$\frac{1}{\sqrt{f_d}} \approx -1.8 \log \left(\left(\frac{\epsilon/D}{3.7} \right)^{1.11} + \frac{6.9}{Re} \right) \quad (\text{Darcy})$$

Frictional pressure loss

$$\Delta P_f = \frac{2}{d_H} f_f \rho u^2 \Delta L \quad (\text{Fanning})$$

$$\Delta P_f = \frac{1}{2d_H} f_f \rho u^2 \Delta L \quad (\text{Darcy})$$

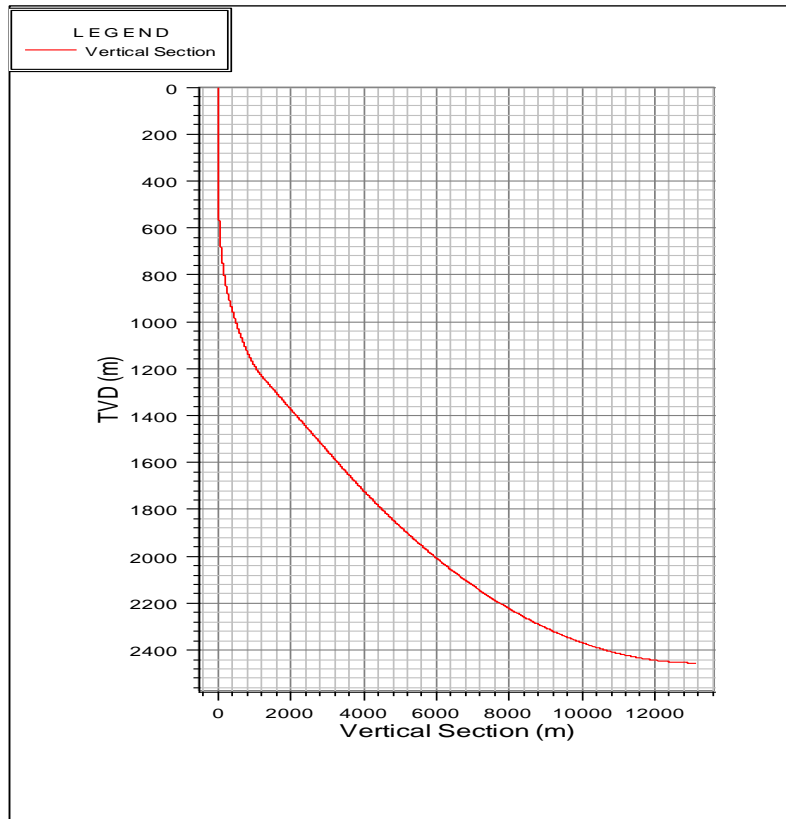
The pressure drop through the nozzles in the drill bit is independent of the type of hydraulic model used. The pressure drop across the bit is defined by the equation:

Appendix B: Simulated well geometry and survey

B1: Survey

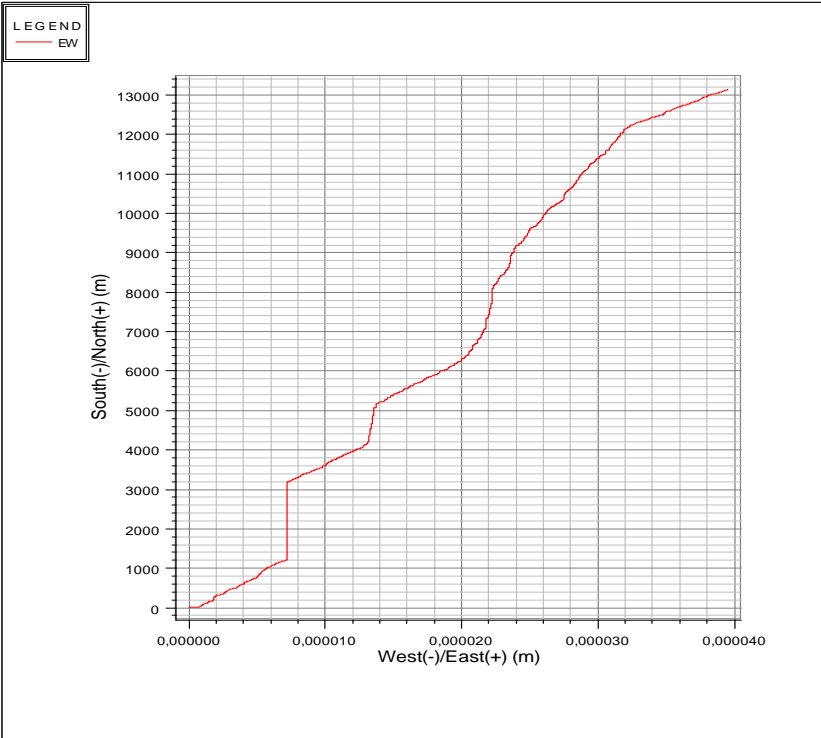
MD (m)	INC (°)	AZ (°)	TVD (m)	DLS (°/100ft)	AbsTort (°/10)	RelTort (°/10)	Vsect (m)	North (m)	East (m)	Build (°/100f)	Walk (°/100f)
100	0	0	100	0	0	0	0	0	0	0	0
200	0	0	200	0	0	0	0	0	0	0	0
300	0	0	300	0	0	0	0	0	0	0	0
400	0	0	400	0	0	0	0	0	0	0	0
500	10	0	499,49	3,05	0,61	0	8,7	8,7	0	3,05	0
600	20	0	595,96	3,05	1,02	0	34,55	34,55	0	3,05	0
700	30	0	686,48	3,05	1,31	0	76,76	76,76	0	3,05	0
800	40	0	768,29	3,05	1,52	0	134,05	134,05	0	3,05	0
900	50	0	838,91	3,05	1,69	0	204,67	204,67	0	3,05	0
1000	60	0	896,2	3,05	1,83	0	286,48	286,48	0	3,05	0
2000	80	0	1236,48	0,61	1,22	0	1221,41	1221,41	0	0,61	0
3000	80	0	1410,13	0	0,81	0	2206,22	2206,22	0	0	0
4000	80	0	1583,78	0	0,61	0	3191,02	3191,02	0	0	0
5000	81	0	1748,82	0,03	0,49	0	4177,3	4177,3	0	0,03	0
6000	82	0	1896,63	0,03	0,42	0	5166,3	5166,3	0	0,03	0
7000	83	0	2027,16	0,03	0,36	0	6157,73	6157,73	0	0,03	0
8000	84	0	2140,36	0,03	0,32	0	7151,29	7151,29	0	0,03	0
9000	85	0	2236,2	0,03	0,29	0	8146,67	8146,67	0	0,03	0
10000	86	0	2314,66	0,03	0,26	0	9143,58	9143,58	0	0,03	0
11000	87	0	2375,71	0,03	0,24	0	10141,7	10141,7	0	0,03	0
12000	88	0	2419,33	0,03	0,22	0	11140,74	11140,74	0	0,03	0
13000	89	0	2445,5	0,03	0,21	0	12140,38	12140,38	0	0,03	0
14000	90	0	2454,23	0,03	0,2	0	13140,33	13140,33	0	0,03	0

B2: Vertical well section

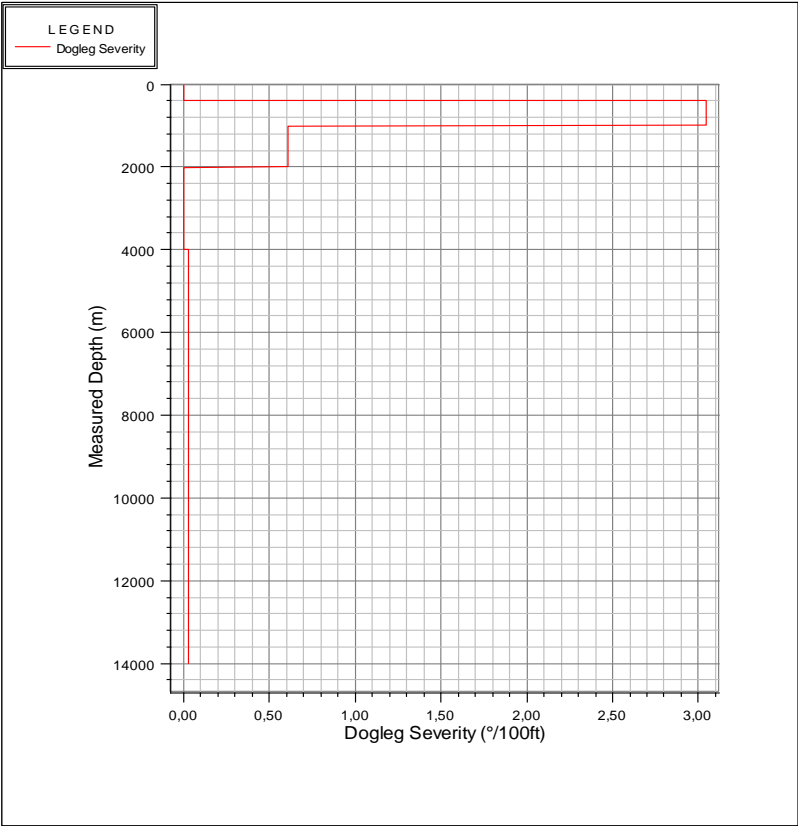


F

B3: Horizontal well section



B4: Dogleg Severity



Appendix C MATLAB code

```
% This will solve pressure loss using Bingham, Power law and Herschel
Buckley flow models''

% =====Input parameters=====

Q600= 134;
Q300 = 76;
Q200 = 56;
Q100 = 39;
Q6= 19;
Q3 = 17;

dw = 12.25;
do = 10.75;
dp = 9.85;

% Bit data

dn1 =28000000000000000000;
dn2 =28000000000000000000;
dn3 =28000000000000000000;

% Surface pressure (back pressure)

DPsrf = 000/14.5;

% flow rate // GPM (gall per minuits) rho = ppg

lr =[];
DP_tot_APIr =[];
DP_tot_HBr =[];

DP_tot_bingr =[];

% Length and density of cement/fluid

%l = 45932;
rho = 10.99;
rho_r=[];
Q=26.4;
for l=0:1000:45932;

%=====
%=====Calculated results=====

PV = Q600-Q300;
YP = Q300-PV;
ty = 1.066*(2*Q3-Q6);

%%%%%%%%%%%%%%%%%%%%%%%%%%%%%%%%%%%%%%%%%%%%%%%%%%%%%%%%%%%%%%%%%%%%%%%%

% Bingham model% Bingham model% Bingham model% Bingham model% Bingham model

%%%%%%%%%%%%%%%%%%%%%%%%%%%%%%%%%%%%%%%%%%%%%%%%%%%%%%%%%%%%%%%%%%%%%%%%
```

```

% velocity
vp_bing_p =0.408*Q/(dp^2);

%apparent viscoicty

mp_bing = Q600-Q300;

ty_bing= Q300-mp_bing;

ma_bing = mp_bing+5*ty_bing*dp/vp_bing_p;

%Reynolds number

Nre_bing_p =928*dp*vp_bing_p*rho/ma_bing;

if Nre_bing_p <2000;

    f_bing_p=16/Nre_bing_p ;

else
    f_bing_p=0.0791/Nre_bing_p ^0.25;
end

% Pressure loss

DP_bing_p = f_bing_p*vp_bing_p^2*rho/25.81/dp;

    DP_bing_p =DP_bing_p*1;

    % In Annulus

vpa_bing_a =0.408*Q/(dw^2-do^2);

ma_bing_a=mp_bing+5*ty_bing*(dw-do)/vpa_bing_a;

    %Reynolds number

Nre_bing_a =757*(dw-do)*vpa_bing_a*rho/ma_bing_a;

if Nre_bing_a <2000;

    f_bing_a=16/Nre_bing_a;

else
    f_bing_a=0.0791/Nre_bing_a^0.25;
end

% Pressure loss

DP_bing_a = f_bing_a*vpa_bing_a^2*rho/25.81/(dw-do);

    DP_bing_a =DP_bing_a*1;

```

```

%////////////////////Total pressure loss Bingham model////////////////////
% Total pressure loss DP = DP_srf + DP_ds + DP_b + DP_a
DP_tot_bing = DP_srf + 0*DP_bing_p + DP_bing_a;
%////////////////////
% Power law model %% Power law model %% Power law model %% Power law model
%
%////////////////////

% velocity
vp_API = 0.408*Q/(dp^2);

%apparent viscoicity
n_API = 3.32*log(Q600/Q300)/2.3026;
k_API = 510*Q300/511^(n_API);
Nre_API_p = 89100*vp_API^(2-
n_API)*rho/k_API*((0.0416*dp)/(3+1/n_API))^(n_API);
Nrec_API_Lam = 3470-1370*n_API;
Nrec_API_Turb = 4270-1370*n_API;
if Nre_API_p < Nrec_API_Lam
    dp_API_p =
k_API*vp_API^(n_API)*((3+1/n_API)/0.0416)^(n_API)/(144000*dp^(1+n_API))*1;
else
    a=(log(n_API)/ 2.3026+3.93)/50;
    b =(1.75-log(n_API)/ 2.3026)/7;
f_API_Turb_p =a/Nre_API_p^b;

dp_API_p = f_API_Turb_p*vp_API^2*rho/25.81/dp*1;
end
% In Annulus
vpa_API_a =0.408*Q/(dw^2-do^2);

%Reynolds number
Nre_API_a = 109000*vpa_API_a^(2-n_API)*rho/k_API*(0.0208*(dw-
do)/(2+1/n_API))^(n_API);

% Critical reynolds number

```

```

Nrec_API_Lam= 3470-1370*n_API;

Nrec_API_Turb= 4270-1370*n_API;

    if Nre_API_p< Nrec_API_Lam

        dp_API_a =
1*k_API*vp_a_API_a^(n_API)*((2+1/n_API)/0.0208)^(n_API)/(144000*(dw-
do)^(1+n_API))

    else

        a=(log(n_API)/ 2.3026+3.93)/50;
        b =(1.75-log(n_API)/ 2.3026)/7;

f_API_Turb_a =a/Nre_API_a^b;

dp_API_a = f_API_Turb_a*vp_a_API_a^2*rho/25.81/(dw-do)*1;

    end

DP_tot_API  = DP_srf + 0*dp_API_p +  dp_API_a;

%////////////////////////////////////

% ==Herschel-Bulkley flow// Herschel-Bulkley flow// Herschel-Bulkley
flow==

%////////////////////////////////////
/

% Pipe flow velocity

vp_HB =0.408*Q/(dp^2);

% Rhelogy parameters from measurnet

n_HB = 0.8492;
k_HB = 0.3267

%tstar_HB= 0.632738399*(0.632738399*Q100+Q6);
%tstar_HB= 0.632738399*(0.632738399*Q100+Q6);

Const_1= (72.25-170.3)/(10.218-170.3)*1.067*(Q6-Q100)+1.067*Q100;

Const_I =Const_1^2-1.067*Q3*1.067*Q600;
Const_II =2*Const_1-1.067*Q3-1.067*Q600;

to_HB = Const_I/Const_II; %6.6582;

%(tstar_HB^2-1.067^2*Q3*Q600)/(2*tstar_HB-1.067*Q3-1.067*Q600);

%Reynolds number

gm = 72.25;

```

```

C = 1- 1/(2*n_HB+1)*(to_HB)/(to_HB+
k_HB*((3*n_HB+1)*Q*0.002228/(n_HB*22/7*(0.5*dp/12)^3))^n_HB);

I1 =2*(3*n_HB+1)/n_HB;

I2 =rho*7.48*vp_HB^(2-n_HB)*(dp/12/2)^n_HB;
I3= to_HB*(dp/12/2/vp_HB)^n_HB+k_HB*((3*n_HB+1)/(n_HB*C))^n_HB;

Nre_pHB =I1*I2/I3;

%Critical values, Nrec

y=(log(n_HB)/log(10)+3.93)/50;
z=(1.75-log(n_HB)/log(10))/7;

Nrec_pHB = (4*(3*n_HB+1)/(n_HB*y))^(1/(1-z));

%friction factor

if Nre_pHB < Nrec_pHB

    dp_pHB = 4*k_HB/14400/(dp/12)*((to_HB/k_HB)+
((3*n_HB+1)/(n_HB*C))*(8*Q*0.002228)/(22/7*(dp/12)^3))^n_HB)*1;

else
    % fhb = y*(C*Nre_HB)^(-z);

    dp_pHB =y*(C*Nre_pHB)^(-
z)*(Q*0.002228)^2*rho*7.48/144/(22/7)^2/(0.5*dp/12)^5*1;

end

% Annular flow velocity

va_HB =0.408*Q/(dw^2-do^2);

Cc = 1- 1/(n_HB+1)*(to_HB)/(to_HB+ k_HB*(2*(2*n_HB+1)/n_HB/((dw/2/12)-
(do/2/12))*Q*0.002228/(22/7*((dw/2/12)^2-(do/2/12)^2)))^n_HB);

Ia1 =4*(2*n_HB+1)/n_HB;

Ia2 =rho*7.48*va_HB^(2-n_HB)*(dw/2/12-do/2/12)^n_HB

Ia3= to_HB*((dw/2/12-
do/2/12)/va_HB)^n_HB+k_HB*(2*(2*n_HB+1)/(n_HB*C))^n_HB;

Nre_aHB =Ia1*Ia2/Ia3;

%Critical values, Nrec

ya=(log(n_HB)/log(10)+3.93)/50;
za=(1.75-log(n_HB)/log(10))/7;

Nrec_aHB = (8*(2*n_HB+1)/(n_HB*ya))^(1/(1-za));

```

```

%friction factor

if Nre_aHB < Nrec_aHB

    dp_aHB = 1*4*k_HB/14400/(dw/12-do/12)*((to_HB/k_HB)+
(16*(2*n_HB+1)/(n_HB*Cc*(dw/12-do/12))*(Q*0.002228)/(22/7*((dw/12)^2-
(do/12)^2)))^n_HB);

    else
        % fhb = y*(C*Nre_HB)^(-z);

        dp_aHB = ya*(Cc*Nre_aHB)^(-
za)*(Q*0.002228)^2*rho*7.48/144/(22/7)^2/(0.5*(dw/12-do/12)^5)*1;

    end

    DP_tot_HB = DP_srf + 0*dp_pHB + dp_aHB;

DP_tot_APIr = [DP_tot_APIr DP_tot_API];
DP_tot_HBr = [DP_tot_HBr DP_tot_HB];
DP_tot_bingr = [DP_tot_bingr DP_tot_bing];
lr = [lr 1];
rho_r = [rho_r rho];

end
rho_static=rho;

figure

% pressure
subplot(2,3,1)
plot(lr*0.3048,DP_tot_bingr/14.7);
title('Frictional Pressure loss. Bingham');
xlabel('Cemented section, m')
ylabel('Frictional pressure loss, s.g')
grid on
drawnow;
hold off

% pressure
subplot(2,3,2)
plot(lr*0.3048,DP_tot_HBr/14.7);
title('Frictional Pressure loss. Herschel Bulkley');
xlabel('Cemented section, m')
ylabel('Frictional pressure loss, s.g')
grid on
drawnow;
hold off

% pressure

subplot(2,3,3)
plot(lr*0.3048,DP_tot_APIr/14.7);
title('Frictional Pressure loss. Power law');
xlabel('Cemented section, m')
ylabel('Frictional pressure loss, s.g')

```

```

grid on
drawnow;
hold off

% pressure ECD
subplot(2,3,4)
plot(lr*0.3048,rho/8.33+DP_tot_bingr/0.052/8051/8.33,
lr*0.3048,rho/8.33,lr*0.3048,15.41/8.33);
title('ECD-Bingham');
xlabel('Cemented section, m')
ylabel('ECD, s.g')
grid on
drawnow;
hold off

% pressure ECD
subplot(2,3,5)
plot(lr*0.3048,rho/8.33+DP_tot_HBr/0.052/8051/8.33,
lr*0.3048,rho/8.33,lr*0.3048,15.41/8.33);
title('ECD-Herschel Bulkley');
xlabel('Cemented section, m')
ylabel('ECD, s.g')
grid on
drawnow;
hold off

subplot(2,3,6)
plot(lr*0.3048,rho/8.33+DP_tot_APIr/0.052/8051/8.33,
lr*0.3048,rho/8.33,lr*0.3048,15.41/8.33);
title('ECD-Power law');
xlabel('Cemented section, m')
ylabel('ECD, s.g')
grid on
drawnow;
hold off

```

Appendix D Review of cementing

Primary cementing

Cementing has been an important part of the oil and gas industry since the first recorded oilfield cementing operation in 1903 by Union Oil Co(Hibbeler, Rae, Gilmore, & Weber, 2000). The cementing operation, in the oil and gas industry, is the process of mixing and placing cement slurry in the annular space between the casing string and the open hole, where the cement slurry will harden and develop its compressive strength

The main objective of primary cementing is to provide zonal isolation of different fluids, i.e., to separate and provide a seal between water or gas in one zone from oil in another zone in the well. To achieve its objective, a hydraulic seal has to be created between the cement and the formations. In addition, there cannot be any fluid channels in the cement sheath. According to Nelson & Guillot, this makes primary cementing the most important operation performed on the well. Other important objectives for the primary cementing are corrosion control and improvement of formation stability and pipe strength (Nelson & Guillot, 2006) (Azar & Samuel, 2007).

Portland Cement

Ordinary Portland Cement (OPC) is by far the most important oilwell binding material in terms of quantity produced, and is used in nearly all well cementing operations. As the term “ordinary” indicates, the cement is manufactured in a rotary kiln from molten matrix of suitably proportioned ingredients. However, as the conditions are significantly different in a well rather than at the surface, special Portland cement are manufactured for use as well cements.

Portland cements is the most common example of a hydraulic cement. Hydraulic cements set and develop compressive strength as a result of hydration by chemical reactions between the water and the compounds in the cement. Setting and hardening of the cement slurry occurs even it's set under water. As the hardened cement has low permeability and is nearly insoluble in water, the cement is an excellent material for zonal isolation.

Two types of raw materials are needed to prepare the mixture that will produce Portland cement clinker: calcareous materials, which contain lime, and argillaceous material, which contain iron oxide, silica and alumina.

Table. D1 Various raw materials used in the manufacture of Portland cement

Calcium	Iron	Silica	Alumina	Sulfate
Alkali waste	Blast-furnace flue dust	Calcium silicate	Aluminum-ore refuse [†]	Anhydrite
Calcite [†]	Clay [†]	Cement rock	Bauxite	Calcium sulfate
Cement-kiln dust	Iron ore [†]	Clay [†]	Cement rock	Gypsum [†]
Cement rock	Mill scale [†]	Fly ash	Clay [†]	
Chalk	Ore washings	Fuller's earth	Copper slag	
Clay	Pyrite cinders	Loess	Fly ash [†]	
Fuller's earth	Shale	Marl [†]	Fuller's earth	
Limestone [†]		Ore washings	Loess	
Marble		Quartzite	Ore washings	
Marl [†]		Rice-hull ash	Shale [†]	
Seashells		Sand [†]	Slag	
Shale [†]		Sandstone		
Slag		Shale [†]		
		Slag		
		Traprock		

[†] Most common sources

The properties of OPC are determined by the mineralogical composition of the clinker. The mineralogical composition of conventional Portland cement clinker is given in **Table 2.2**. However, for special cements, the content of aluminate and ferrite phase may differ significantly (Nelson & Guillot, 2006).

Table D.2. Mineralogical composition of classic Portland cement clinker

Oxide Composition	Cement Notation	Common Name	Concentration (wt%)
$3\text{CaO} \cdot \text{SiO}_2$	C_3S	Alite	55–65
$2\text{CaO} \cdot \text{SiO}_2$	C_2S	Belite	15–25
$3\text{CaO} \cdot \text{Al}_2\text{O}_3$	C_3A	Aluminate	8–14
$4\text{CaO} \cdot \text{Al}_2\text{O}_3 \cdot \text{Fe}_2\text{O}_3$	C_4AF	Ferrite phase	8–12

Cement additives

Cement additives is used to modify the Portland cement to required properties. Temperature can be below freezing point in permafrost zone, while the pressure can range from near ambient in shallow wells to more than 2,000 bar in deep wells. In addition, the cement must often be designed to contend with weak or porous formations, corrosive fluids, and overpressured formation fluids. The goal of the cement additives is to design the cement

slurry to allow a successful slurry placement between the casing and the formation, rapid compressive strength development, and adequate zonal isolation during the lifetime of the well.

Today there exist more than 100 additives for well cementing. The eight major categories are:

- Accelerators: chemicals that shorten the setting time of the cement slurry and increase the rate of compressive strength development.
- Retarders: chemicals that delay the setting time of the cement system.
- Extenders: materials that lower the density of a cement system reduce the quantity of cement per unit volume of set product, or both.
- Weighting agents: materials that increase the density of the cement system.
- Dispersants: chemicals that reduce the viscosity of the cement slurry.
- Fluids loss control agents: materials that control loss of the cement slurry to weak or porous/vugular formations.
- Specialty additives: miscellaneous additives, such as antifoam agents, fibers, and flexible particles (Nelson & Guillot, 2006).

Running and cementing the casing

The casing must be run in the hole in an efficient and smooth manner to ensure a safe operation. If there is a pause in the running procedure, the casing may be stuck and impossible to move again. As the casing is of a larger diameter than the drill string, the annular clearance is smaller and the displacement and surge pressures in the annulus usually are higher when running the casing rather than the drill string in the hole, it is important to limit the running speed of the casing. Minimizing the surge pressure will reduce the risk of fracturing the formation. If the formation is fractured during the running operation, the risk of differentially sticking the casing off bottom is increased, and the chances of getting a good cement job is usually decreased considerably (Byrom, 2007).

This part describes a typical procedure for a single-stage primary cement job. From bottom to top the casing string may consist of:

- **Guide/float shoe** is first item of the casing string and its purpose is to direct the casing smoothly into the hole, minimize well-side cavings and ensure a safe passing through crooked holes.
- **Float collar** is installed if the guide shoe does not have a float. The main purpose of the float collar is to prevent the cement from flowing back into the casing.
- Several **Centralizers** attached along the section that is to be cemented to keep the casing off the borehole wall and centralize it as much as possible. A centralized casing provide a uniform fluid-flow profile around the annulus, which is important to ensure a good drilling-fluid removal and a proper cement placement.
- **Scratchers** attached along the casing string to remove loose filter cake. Scratchers are most effective while the cement is being pumped. Like centralizers, scratchers help to distribute the cement around the casing. There are two general types of scratchers,

those that are used when the casing is rotated, and those that are used when the casing is moved up and down the wellbore.

The next step is to install the cementing head and attach it to the joint of the casing. The cementing head allows cementing plugs to be run ahead and behind the cement slurry, to isolate the cement slurry from wellbore fluids in front of the plug, and displacement fluid behind the cement slurry. The plugs have wiping fins to mechanically clean the well.

When the casing is at the bottom, the well is normally circulated to remove gelled drilling fluid and make it mobile. This step is very important since it is more difficult to remove the drilling fluid from the narrow annulus around the casing. As the drilling fluid may be severely gelled since it has been static in the well for several hours, the circulation is normally broken slowly to prevent formation fractures. Moving the casing string will improve the gelled-drilling-fluid removal and help the flow go into the narrow side of the annulus. A preflush may also be used. The preflushes are used to thin and disperse drilling-fluid-artichles, and are usually gone into turbulent flow at low flow rates to help the cleaning of the well. Some chemical preflushes aggressively attack specific drilling fluids and breaking them down for enhanced drilling-fluid removal.

A spacer may be pumped between the drilling fluid and the cement slurry. A spacer is used to avoid mud contamination in the cement. A spacer may also be used to enhance the removal of gelled drilling fluid or weighted spacer can help with well control. It is very important that the drilling fluid/spacer interface and the spacer/cement slurry interface are compatible.

The cement slurry is then pumped down casing between the two plugs. When the bottom plug reaches the float collar, it stops and pressure builds up quickly until the bottom plug's diaphragm ruptures and allows the slurry to continue. The top plug, however, has a solid core and will not rupture by the pressure buildup when the top plug reaches the float collar. The position of the top plug may be determined by calculating the fluid displacement, as the casing volume is known, or by using a measuring wire. The pressure buildup is also a sign that the plugs have reached the float collar. The casing between the guide shoe and float collar is filled with cement and can be drilled out if necessary (Mitchell & Miska, 2011).